January 2020

Synthesis And Characterization Of Lignin Nanoparticles For Potential Applications In Advanced Sustainable Materials

Steven Chandler Borrillo

SYNTHESIS AND CHARACTERIZATION OF LIGNIN NANOPARTICLES FOR POTENTIAL APPLICATIONS IN ADVANCED SUSTAINABLE MATERIALS

by

Steven Chandler Borrillo

Bachelor of Science, University of North Dakota, 2018

A Thesis

Submitted to the Graduate Facility

of the

University of North Dakota

In partial fulfillment of the requirements

For the degree of

Master of Science

in

Mechanical Engineering

Grand Forks, North Dakota

August

2020

RESERVED FOR PROQUEST PAGE

Name: Steven Chandler Borrillo

Degree: Master of Science

This document, submitted in partial fulfillment of the requirements for the degree from the University of North Dakota, has been read by the Faculty Advisory Committee under whom the work has been done and is hereby approved.

DocuSigned by:
Surojit Gupta
Surojit Gupta

DocuSigned by:
Clement Tang
Clement Tang

DocuSigned by:
Yun Ji
Yun Ji

This document is being submitted by the appointed advisory committee as having met all the requirements of the School of Graduate Studies at the University of North Dakota and is hereby approved.

DocuSigned by:
Chris Nelson
Chris Nelson
Dean of the School of Graduate Studies

8/11/2020
Date

PERMISSION

Title	Synthesis and Characterization of Lignin Nanoparticles for Potential Applications in Advanced Sustainable Materials
Department	Mechanical Engineering
Degree	Master of Science

In presenting this thesis in partial fulfillment of the requirements for a graduate degree from the University of North Dakota, I agree that the library of this University shall make it freely available for inspection. I further agree that permission for extensive copying for scholarly purposes may be granted by the professor who supervised my thesis work or, in his absence, by the Chairperson of the department or the dean of the School of Graduate Studies. It is understood that any copying or publication or other use of this thesis or part thereof for financial gain shall not be allowed without my written permission. It is also understood that due recognition shall be given to me and to the University of North Dakota in any scholarly use which may be made of any material in my thesis.

Name: Chandler Borrillo

Date: 08/09/2020

TABLE OF CONTENTS

LIST OF FIGURES…… ix

LIST OF TABLES…….. xi

ACKNOWLEDGEMENTS…… xii

ABSTRACT……. xiii

CHAPTER I: INTRODUCTION…….. 1

1.1 Background and Motivation…… 1

1.2 Biopolymer Solution……... 2

1.3 Lignin Structure and Sources…… 2

1.4 Lignin Properties, Benefits, and Applications…… 4

1.5 Lignin Potential to Improve Mechanical Properties……... 5

1.6 Organization of Thesis…… 6

CHAPTER II: DESIGN AND CHARACTERIZATION OF LIGNIN BIOPLASTIC COMPOSITES FROM LIGNIN-ACETONE SOLUTION…… 7

2.1 Introduction……. 7

2.2 Experimental Details……... 7

2.2.1 Manufacturing Process for Designing Lignin-Acetone Solution…… 7

2.2.2 Solubility of Lignin in Acetone…… 9

2.2.3 Design of Lignin Reinforced Bioplastics by Solvent Casting…… 9

2.2.4 Design Matrix of Composition…… 11

2.2.5 FTIR, TGA, and DSC Characterization……... 12

2.2.6 Tensile Testing……. 12

2.3 Results and Discussion…… 13

2.3.1 Solubility Studies……. 13

2.3.2 FTIR, TGA, and DSC…….. 15

2.3.3 Tensile Strength…….. 18

2.4 Conclusions…… 25

CHAPTER III: DESIGN AND CHARACTERIZATION OF LNP FROM LIGNIN-WATER SOL……... 26

3.1 Introduction……. 26

3.2 Experimental Details……... 26

3.2.1 Manufacturing Process……. 26

3.2.2 Particle Size Characterization…….. 28

3.2.3 Zeta Potential Characterization…… 29

3.2.4 SEM Analysis of Nanoparticles……... 30

3.2.5 ImageJ Analysis of SEM Characterization…….. 30

3.3 Results and Discussion…… 30

3.3.1 DLS…….. 30

3.3.2 Zeta Potential, Mobility, and Conductivity…….. 31

3.3.3 SEM Analysis of Nanoparticles…….. 33

3.4 Conclusions……. 36

CHAPTER IV: DESIGN AND CHARACTERIZATION OF LIGNIN COATINGS.. 37

4.1 Introduction……. 37

4.2 Experimental Design……... 37

4.2.1 Manufacturing Process……. 37

4.2.2 Optical Microscopy, SEM, Wettability, and Vickers Hardness Characterization…... 38

4.3 Results and Discussion…… 38

4.3.1 Optical Microscopy…….. 38

4.3.2 SEM…….. 39

4.3.3 Wettability…… 42

4.3.4 Vickers Hardness……. 43

4.4 Conclusions……. 44

CHAPTER V: DESIGN OF ULTRASONIC SPRAY SET UP AND FUTURE WORK…….. 45

5.1 Introduction……. 45

5.2 Experimental Design……... 45

5.2.1 Manufacturing Process……. 45

5.2.2 Design Matrix……... 47

5.3 Discussion and Future Work……... 47

REFERENCES…….. 49

LIST OF FIGURES

Figure 2.1: (a) 5 g of lignin in a glass container, and (b) lignin particles in acetone (before stirring).

Figure 2.2: Procedure to create lignin-acetone solution.

Figure 2.3: Procedure to solvent cast lignin bioplastic composites.

Figure 2.4: Schematics of dog-bone samples [17].

Figure 2.5: Lignin was partially dissolved in acetone after stirring for, (a) 2 h, (b) 24 h, (c) precipitation of nano-lignin by adding DI water, and (d) formation of lignin coating on glass surface after drying [picture courtesy: Dr. S. Gupta].

Figure 2.6: Solubility of lignin in acetone versus time.

Figure 2.7: (a) FTIR (400-2000 cm^{-1}), (b) FTIR (2000-4000 cm^{-1}), (c) TGA, and (d) DSC analysis of indulin and lignin-acetone.

Figure 2.8: DSC plot of, (a) CA-lignin, (b) PLA-lignin (second heating cycle), (c) PHA-lignin (second heating cycle), (d) PLA-PHA-lignin (second heating cycle).

Figure 2.9: Plot of tensile stress versus displacement of (a) CA-lignin, (b) PLA-lignin, (c) PHA-lignin, and (d) 50%-50% PLA-PHA-lignin blends.

Figure 2.10: Plot of tensile strength of different blends as a function of lignin concentration.

Figure 2.11: SE SEM micrographs of, (a) CA-3 vol% lignin, (b) CA-3 vol% lignin (higher magnification), (c) CA-9 vol% lignin, (d) CA-9 vol% lignin (higher magnification), (e) PLA-3 vol% lignin, (f) PLA-3 vol% lignin (higher magnification), (g) PLA-9 vol% lignin, (f) PLA-9 vol% lignin in BSE.

Figure 2.12: SEM micrographs of, (a) PHA-3 vol% lignin, (b) PHA-3 vol% lignin (higher magnification), (c) PHA-9 vol% lignin, (d) PHA-9 vol% lignin (higher magnification), (e) PLA-PHA-3 vol% lignin, and (f) PLA-PHA-3 vol% lignin (higher magnification), (g) PLA-PHA-9 vol% lignin, and (h) PLA-PHA-9 vol% lignin (higher magnification).

Figure 3.1: Procedure to create lignin-water sol.

Figure 3.2: Plot of intensity versus particle size of, (a) HTS5-19-10 (water), (b) HTS5-19-11 (water), and (c) HTS5-19-12 (water).

Figure 3.3: Plot of, (a) zeta potential, (b) mobility, (c) conductivity, and (d) zeta potential (stability) as a function of lignin concentration in the solution.

Figure 3.4: SEM of, (a) HTS5-29-1, (b) HTS5-29-1 (higher magnification), (c) HTS5-29-2, (d) HTS5-29-2 (higher magnification), (e) HTS5-29-3, (f) HTS5-29-3 (higher magnification), (g) HTS5-29-4, (h) HTS5-29-4 (higher magnification), (i) HTS5-29-5, (j) HTS5-29-5 (higher magnification), (k) HTS5-29-6, and (l) HTS5-29-6 (higher magnification).

Figure 4.1: (a) lignin-acetone coated stainless-steel, (b) stainless-steel, (c) lignin-acetone coated mica, (d) as-received mica, (e) lignin-acetone coated Corning glass, and (f) as-received Corning glass.

Figure 4.2: Optical microscopy at 10X magnification of (a) as-received mica, and (b) lignin-acetone coated mica (c) as-received Corning glass, (d) lignin-acetone coated Corning glass, (e) as received stainless-steel, and (f) lignin-acetone coated stainless-steel.

Figure 4.3: SEM micrographs of, (a) dried and crushed lignin-acetone, (b) dried and crushed lignin-acetone at higher magnification, (c) as-received mica, (d) lignin-acetone coated mica, (e) as-received stainless-steel, (f) lignin-acetone coated stainless-steel, (g) as-received Corning glass, and (h) lignin-acetone coated Corning glass.

Figure 4.4: Water droplet on as-received, (a) mica, (b) Corning glass, and (c) stainless steel, and lignin-acetone coated surface of, (d) mica, (e) Corning glass, and (f) stainless steel.

Figure 4.5: Optical microscopy of Vickers hardness indentation with a 0.3 kg load for 15 seconds of (a) stainless-steel at 50X, (b) stainless-steel lignin coated at 10X, (c) stainless-steel lignin coated at 50X, (d) mica substrate at 50X, (e) mica lignin coated at 10X, (f) mica lignin coated at 50X, (g) Corning glass substrate at 50X, (h) Corning lignin coated at 10X, and (i) Corning lignin coated at 50X.

Figure 5.1: Atomizer nozzle attached to an ultrasonic power supply and syringe with a syringe pump.

Figure 5.2: Experimental setup to deposit LNPs with an ultrasonicator.

LIST OF TABLES

Table 2.1: Different compositions designed during this study (student collaborators: Nicholas Johnson and Maharshi Dey)

Table 2.2: Analyzed lignin bioplastic samples based on volume percentage of lignin

Table 3.1: Composition of lignin-acetone solution

Table 3.2: Volume percentage of lignin in a lignin-water sol for each sample

Table 3.3: Particle size of lignin in a lignin-water sol

Table 3.4: Particle size of LNP on Al stud measured using ImageJ analysis of SEM

ACKNOWLEDGEMENTS

Chapter 2 was funded by NSF EPSCoR and Dean Professorship. Students Nicholas Johnson and Maharshi Dey helped me with the sample fabrication and characterization. Chapters 3 and 4 were funded by the ME Department and Dean Professorship. I had performed initial experimentation. However, due to COVID-19, my travel from Minnesota to North Dakota was restricted, so Dr. S. Gupta completed the manufacturing and characterization experiments. We had regular meetings to brainstorm and discuss results.

I would like to thank the rest of my colleagues who assisted indirectly towards to completion of this thesis. I would also like to thank the countless professors I have had throughout six years of schooling at UND. I extend my sincere appreciation to my advisor, Dr. S. Gupta. His captivating lectures compelled me to take up an interest in materials.

Finally, I thank all my friends and family for their support throughout the years during my schooling.

ABSTRACT

It is no surprise to most that the use of petroleum-based plastics has caused environmental challenges at a global scale. A large percentage of plastic waste is disposed in the natural environment while a small portion of that is biodegradable. One promising solution to tackling the worlds' dependency on non-renewable plastics is the development of alternative materials such as bioplastics. A few popular biopolymers include Polylactic Acid (PLA), Polyhydroxyalkanoate (PHA), and Cellulose Acetate (CA) which boast properties such as biodegradability, sourced from renewable resources, and non-toxicity. In addition, lignin is worth researching as a biopolymer because it is naturally occurring, biodegradable, biocompatible, and has potential as a structural additive. Lignin may be processed to form lignin nanoparticles which takes advantage of greater interfacial bond strength due to an increase in surface area to volume ratio.

In this thesis, we are reporting a method for extracting a fraction of lignin which is soluble in acetone. By using this soluble fraction, we have fabricated and characterized lignin reinforced bioplastics, lignin nanoparticles (in sol and particle form), and coatings on different substrates. In addition, we are proposing a method by using these solutions and their derivatives which have the potential to be deposited using a ultrasonicator sprayer.

CHAPTER I: INTRODUCTION

1.1 Background and Motivation

With the turn of the 20th century, the very first synthetic polymer was invented, known as Bakelite [1]. Throughout the next century, petroleum-based polymers exploded in popularity and crept their way into almost every aspect of life. It is well known that plastics can be engineered for a wide variety of applications at a fraction of the price of alternative materials. Some applications may be lifesaving, such as economical water storage and personal protective equipment. However, many applications of plastic are used in a wasteful manner, such as disposable kitchenware. Since 1950, more than 1 ton of plastic has been created per person alive today [2]. A staggering 60 percent of that waste is disposed of in our natural environment either in landfills or as lost litter [2]. Less than one percent of plastics are sourced from renewable resources [2]. The overwhelming majority of plastics are sourced from inorganic polymers, which presents a grave challenge to society in disposal due to plastic having poor biodegradability. Depending on the type of plastic, most petroleum-based plastics take anywhere from a few hundred to a thousand years to decompose.

The issue that our society is consuming plastic faster than the world may sustain and decompose presents one further question to researchers and industry: why make the change now? The development of products and services which reduce environmental impact has become a winning business strategy for small and large corporations a like. According to a 2017 Forbes study, 92% of Americans would be more likely to trust a company that supports a social or environmental issue [3]. People are more willing than ever to change their spending habits and lifestyles to encourage environmental sustainability. This is a result of consistent public education. Progress towards global sustainability has been challenged by many industries that rely and utilize

petroleum-based materials to contribute towards their bottom dollar. While scientific discovery for societal advancement is a key driver of many new technologies, it is humanities' duty to care for the environment for the generations to come.

1.2 Biopolymer Solution

While our societal dependency on petroleum-based products is a complex issue to resolve, most scientists can agree that a combination of solutions will be required to tackle this challenge. Before the turn of the 21st century, a campaign was launched to address the environmental destructiveness of societies addiction to plastic: reduce, reuse, recycle. While this solution has kicked off the necessary conversation between manufacturers and consumers, the reality is that our society still relies heavily on petroleum-based products.

A second solution to reducing dependency on petroleum-based plastics is the development of alternative materials. There are multiple materials already in production with many more currently being developed. A few popular plastic materials made from renewable resources include Polylactic Acid (PLA), Polyhydroxyalkanoate (PHA), and Cellulose Acetate (CA). Biopolymers such as these are biodegradable, may be created from renewable resources, and are often non-toxic to humans. One such promising material that will be discussed next is the use of lignin in biopolymers.

1.3 Lignin Structure and Sources

Lignin is a highly branched three-dimensional natural polymer found in most plant structures alongside hemicellulose and cellulose [4]. Lignin is often found in the outermost layer of a plant structure acting as a binding agent, microbial barrier, and structural support in the plant cell walls [5]. It can also be found in the interior of the plants' structure acting as a binding agent while cellulose acts as the interior structural component. Lignin has polyphenol structure

composed of three different phenylpropane units: Guaiacyl (G), Syringyl (S), and P-hydroxyphenyl (H) [5]. Each of these units differ by the degree of substitution of methoxyl groups in the aromatic ring. Depending on the plant matter, the phenylpropane units present vary. For example, wood may be commonly composed of a combination of Guaiacyl and Syringyl units while grass may have a combination of Guaiacyl, Syringyl, and P-hydroxyphenyl [6].

Before moving on to a description of the sources of lignin, there are a couple of key take-aways regarding processing and utilizing lignin. First, solubility of lignin is pH sensitive, for example industrial sulfate lignin can be dissolved in NaOH while the pH is maintained at ~13 [7]. Most processing techniques include the use of acids or bases to alter the aqueous solution used during fabrication and alteration. Secondly, solubility of lignin in different solvents can be used to generate nanoparticles [8]. This will play an important role in designing composite biopolymers.

As was mentioned previously, lignin is a key component found within plant structures. A few examples of plants high in lignin concentration include wood pulp, jute, hemp, and cotton. The potential for use of lignin as a biopolymer is great because lignin is an abundant natural polymer often found in agricultural waste products. One common source of concentrated lignin is a by-product of the paper making industry. Paper is produced from processing wood into a pulp. Processing methodologies such as kraft, sulfite, and alkaline pulping processes are used to remove lignin from the cellulose dense pulp [9]. The resulting by-product is known as black liquor which is both rich in lignin and has a high energy density. The lignin extracted from black liquor is commonly referred to as industrial lignin, or alkali lignin, due to the use of basic solutions during processing. In the kraft lignin purification process, precipitation and ultrafiltration using ceramic membranes is used to process black liquor into isolated lignin [9]. One downside to kraft lignin is

that prior to use, it often requires additional chemical processes such as alkylation, or acetylation, for increasing compatibility with non-polar polymer matrices [6].

1.4 Lignin Properties, Benefits, and Applications

Depending on the processing method, lignin has the potential to have an abundant number of functional groups [6, 10]. Functional groups such as phenolic, carboxylic, and aliphatic hydroxyl groups allow for chemical modification and polarity adjustment [6, 10]. These groups lead towards good matrix compatibility that aid in designing biopolymers and composite materials. Acid and bases may be used to tailor the properties of lignin structures due to their impact on the availability of functional groups within the structure [6]. These chemical treatments can increase the expense of reutilizing of lignin thus novel processes are required to valorize lignin based functional materials.

A handful of other properties lignin possesses include that it is naturally occurring, biodegradable, biocompatible, antimicrobial, hydrophobic, reinforcing, plasticizing, and UV absorbing [6, 10].

To give a little bit of context for the abundancy of lignin, according to Christopher et al. [11], the paper and pulp industry produces approximately 50-60 million tons of lignin on an annual basis. With a valuation set at $0.18/kg, the value of the waste product is approximately $300 million. If a method is developed to valorize all the lignin by-product, the market would be an estimated $12-35 billion dollars, nearly 100 times greater [11].

Due to the afore mentioned properties, lignin has a wide variety of applications. Some of the applications include functional surface coatings, natural rubber additives, drug delivery and wound healing in biomedical applications, antimicrobial materials, UV or thermo-oxidation protection in various polymers, and wastewater treatment [6, 10].

1.5 Lignin Potential to Improve Mechanical Properties

While cellulose is a promising mechanical strengthening additive in composite materials, lignin has not had the same success. Previous attempts to add lignin as a polymer additive to form next generation composite materials resulted in degraded mechanical properties. Earlier when it was mentioned that during the pulping process to produce paper, lignin is mechanically or chemically removed from the pulp. The main reason cellulose is separated from lignin is that cellulose has greater mechanical properties, so removing the lignin from the pulp will enhance the strength of the paper. Black liquor is both abundant and has few methods to valorize it.

Recent research has shown that lignin can be used design biofoams [12]. The interest of the research presented here is further focused on a niche use of lignin: as a nanoparticle. The main advantage of using lignin nanoparticles (LNP) over micro-sized lignin particles primarily lies in the fact that as a nanoparticle, interfacial bond strength is greatly improved due to the increase in surface area to volume ratio. Nano technology is still a relatively new field of study with many more discoveries to be made. Learning how to design and manufacture nanoparticles still challenges scientists, especially at an industrial scale. Characterization of nanoparticles is often tedious, time consuming, and requires highly precise equipment.

Dong et al. [4] used dimethylsulfoxide (DMSO) to dissolve technical lignin and then used dialysis to precipitate LNPs. By using direct light scattering (DLS), they measured lignin nanoparticles in the range of 195-197 nm. Yang et al. [13] designed nanoparticles by treating a solution of 4% wt. of lignin in ethylene glycol by HCl. They obtained lignin nanoparticles of particle size 48.85 ± 16.38 nm by using this method. Reference [14] has summarized details of other procedures for fabricating LNPs. In this thesis, we will explore novel methodologies of reutilizing and valorizing lignin.

1.6 Organization of Thesis

Following the introductory chapter, four additional chapters have been written to further describe the design and characterization of lignin nanoparticles for potential applications in advanced sustainable materials. Chapter II describes the design and characterization of lignin bioplastic composites from lignin-acetone solution. Lignin-acetone solution has been characterized using a variety of methods including Fourier-transform infrared spectroscopy (FTIR), thermogravimetric analysis (TGA), and differential scanning calorimetry (DSC). Lignin bioplastic composites have been fabricated utilizing lignin-acetone solution. Lignin reinforced bioplastic composite materials were characterized using DSC, tensile testing, and scanning electron microscopy (SEM).

Chapter III describes the design of lignin-water sol, which builds upon the methodology to produce lignin-acetone solution described in chapter II. Lignin-water sol is characterized using dynamic light scattering (DLS) as well as a zeta potential analyzer, which also reports mobility and conductivity. Additionally, chapter III describes the fabrication of solid lignin nanoparticles derived from the lignin-water sol. The LNP SEM images were characterized by using ImageJ.

Chapter IV details the design and characterization of lignin coatings. In this chapter, drip coatings were synthesized and characterized by using optical microscopy, SEM, wettability analysis, and Vickers hardness.

Finally, chapter V describes a novel method to deposit LNPs onto a substrate using an ultrasonic sprayer. The characterization of LNPs deposited using the ultrasonic spray methodology is a part of the future work.

CHAPTER II: DESIGN AND CHARACTERIZATION OF LIGNIN BIOPLASTIC COMPOSITES FROM LIGNIN-ACETONE SOLUTION

2.1. Introduction

It is difficult to design polymer composites by using lignin as it has issues with melt processing [6]. Like discussed in the last section, incorporating lignin in a non-polar matrix is non-trivial due to its polymeric structure [6]. For example, Anwer et al. [15] and Oihana et al. [16] have reported deterioration in strength of Poly Lactic Acid (PLA) after the addition of lignin particles in the polymer matrix. Recently, Aldam et al. [17] reported synthesis and characterization of binary and ternary blends of Poly Hydroxy Alkanoate (PHA), PLA, and Cellulose Acetate (CA). In this chapter, we will report the synthesis and characterization of bioplastics by using extracted lignin as additives.

2.2 Experimental Details

2.2.1 Manufacturing Process for Designing Lignin-Acetone Solution

The first step used to prepare the lignin-acetone solution was to dissolve ~5 g of lignin (Indulin AT, MeadWestvaco, Richmond, VA) in 50 mL of acetone (grade: for HLPC ≥99.9%, Sigma Aldrich, St. Louis, MO) in a glass jar (VWR Tall Jar, VWR International LLC., Radnor, PA) with a phenolic lid with a PTFE/LDPE Liner. Next, a Teflon coated medium-sized magnetic stirrer was added to the glass jar and the lid was closed to prevent the slow evaporation of acetone into the atmosphere. The glass jar was placed on a magnetic stir plate set to a medium speed for a specified amount of time at room temperature, as shown in Figure 2.1.

Figure 2.1: (a) 5 g of lignin in a glass container, and (b) lignin particles in acetone (before stirring).

During this experiment, we stirred the samples for 2, 24, and 72 h. Once the stirring was completed, the lignin solution was then poured into three 15 mL glass centrifuge tubes. The slurry was then centrifuged (Unico Powerspin Lx) at 3,000 rpm for 5 min. The soluble portion was then decanted into a new glass container, leaving behind the insoluble portion in the glass centrifuge tube. Figure 2.2 illustrates the full procedure to create lignin-acetone solution.

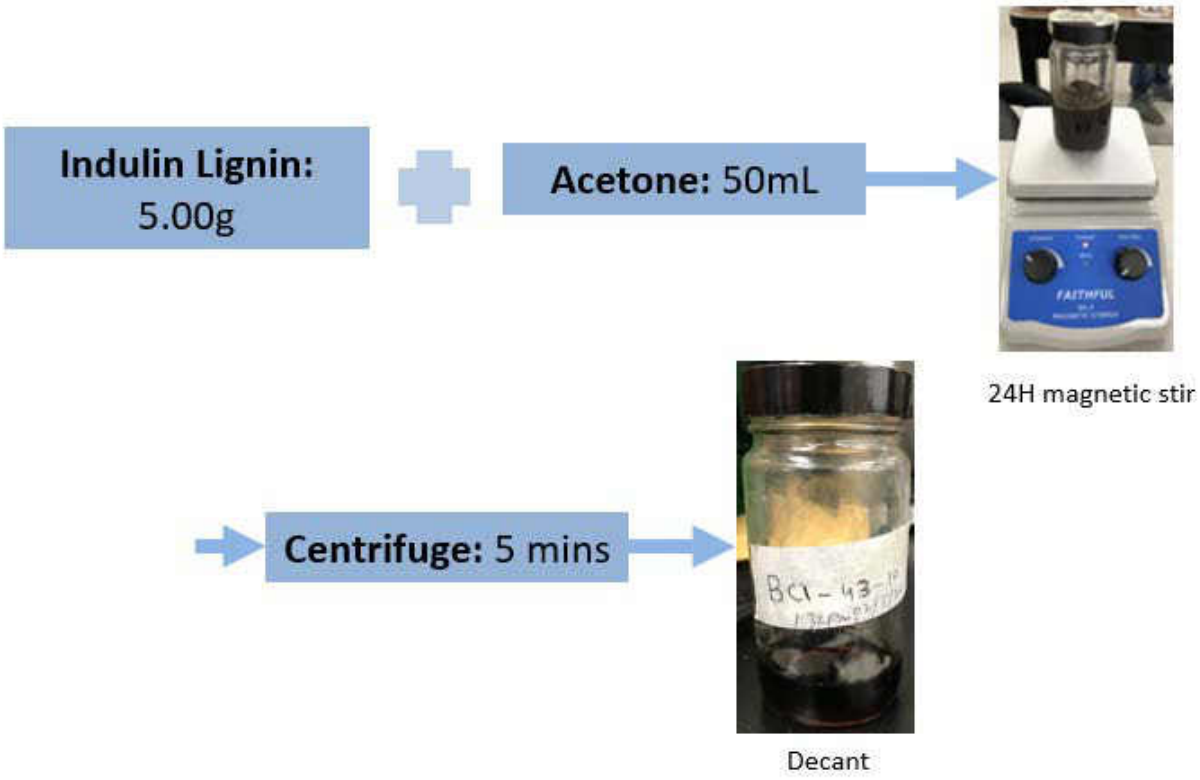

Figure 2.2: Procedure to create lignin-acetone solution.

2.2.2 Solubility of Lignin in Acetone

A solubility study was performed to determine the duration required to dissolve an alkali lignin in an organic solvent. In addition to Indulin Lignin, alkali lignin (Part Number 370959, Sigma Aldrich, St. Louis, MO) was also used during the study. For determining solid content, dissolved lignin in solvent was poured into three separate glass containers; thereafter, the samples were dried at 100 ºC for 5 h. The mass of residual lignin was used to calculate the solid fraction dissolved in lignin.

2.2.3 Design of Lignin Reinforced Bioplastics by Solvent Casting

Solvent casting was the manufacturing process used to create lignin reinforced bioplastic samples described in Table 2.1. To start, 5 g of bioplastic material was measured and added to 50 mL of organic solvent in a glass container. Acetone was used as the organic solvent for CA while

Dichloromethane (DCM) (anhydrous, ≥99.8%, contains 40-150 ppm amylene as stabilizer; Sigma Aldrich, St. Louis, MO), was used to dissolve PHA and PLA. These organic solvents were chosen based on their effectiveness for dissolving the respective bioplastic material. Next, a Teflon coated medium-sized magnetic stirrer was added to the glass jar and the lid is closed. The glass jar was then placed on a magnetic stir plate set to a medium speed for approximately 24 h while at room temperature.

Table 2.1: Different compositions designed during this study (student collaborators: Nicholas Johnson and Maharshi Dey)

<table>
<tr><th>Lignin-Acetone (ml)</th><th>CA-Acetone (ml)</th><th>PLA-DCM (ml)</th><th>PHA-DCM (ml)</th><th>PLA-PHA-DCM (ml)</th></tr>
<tr><td>2</td><td>23</td><td rowspan="2">x</td><td rowspan="4">x</td><td rowspan="6">x</td></tr>
<tr><td>5</td><td>20</td></tr>
<tr><td>2</td><td rowspan="6">x</td><td>23</td></tr>
<tr><td>5</td><td>20</td></tr>
<tr><td>2</td><td rowspan="4">x</td><td>23</td></tr>
<tr><td>5</td><td>20</td></tr>
<tr><td>2</td><td rowspan="2">x</td><td>23</td></tr>
<tr><td>5</td><td>20</td></tr>
</table>

Once the bioplastic is dissolved in the organic solvent, a previously prepared lignin solution was measured and added to a measured amount of dissolved bioplastic. Table 2.1 shows different compositions fabricated during this study. The volume concentration of each constituent was measured by using a graduated glass cylinder. The lignin-acetone solution and dissolved solution was magnetically stirred in a new glass container at room temperature for approximately 5 min. Once the end solution appears visually homogenous, it was removed and poured into a Teflon coated muffin pan to solvent cast the samples. Approximately ~8 g of solution was added to each muffin slot. Once poured, the samples were placed aside at room temperature to set for 24 h while the organic solvent evaporated. Once dry, the samples were placed into an oven for 24 h at 100 °C. For tensile testing, dog-bone shape sample was cut before placing the sample into the oven

since the samples become difficult to machine after heat treatment. When the samples exited the oven, they were bone-dried for characterization. Figure 2.3 below depicts the overall procedure for creating lignin bioplastic composites.

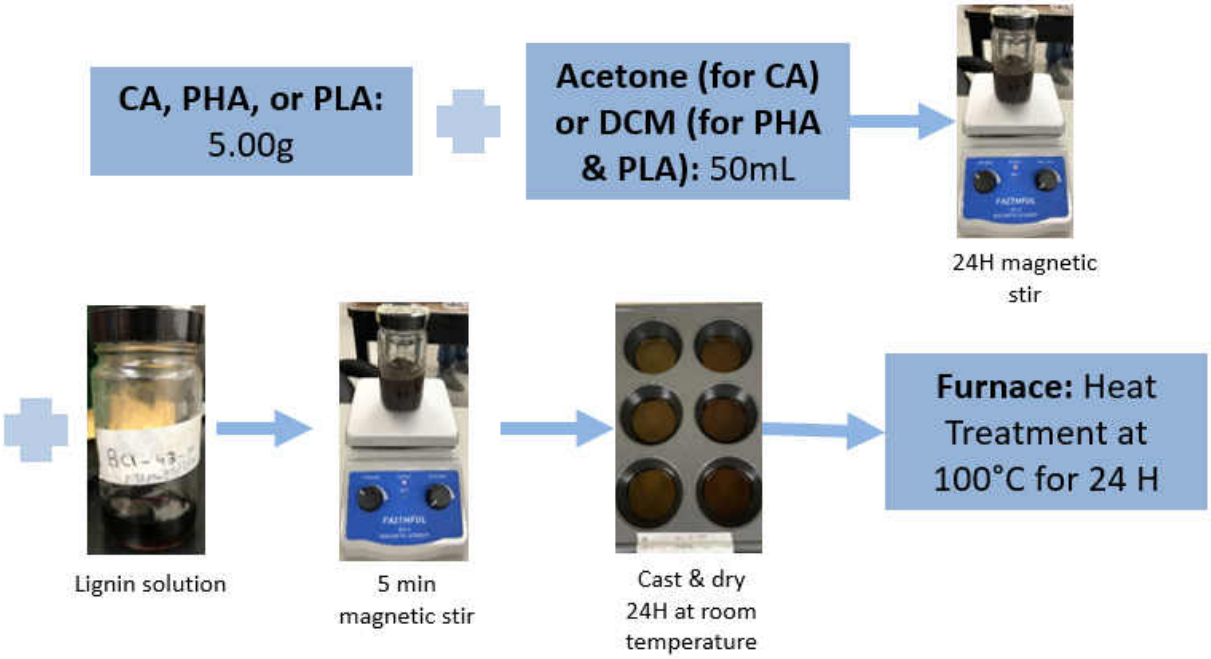

Figure 2.3: Procedure to solvent cast lignin bioplastic composites.

2.2.4 Design Matrix of Composition

A total of 12 different samples were created for analysis. Table 2.2 illustrates the sample compositions in vol% based on Table 2.1 (please note, density of as-received indulin lignin was used to calculate the volume fraction). The density of different constituents was used to calculate the respective volume fraction of each composition.

Table 2.2: Analyzed lignin bioplastic samples based on volume percentage of lignin

Bioplastic	**Volume Percentage of Lignin (%)**		
CA	0	3.3	9.2
PLA	0	3.3	8.8

PHA	0	3.3	8.9
PLA-PHA	0	3.3	8.8

2.2.5 FTIR, TGA, and DSC Characterization

Fourier transform infrared spectroscopy (FTIR), thermogravimetric analyzer (TGA), and Differential Scanning Calorimetry (DSC) were performed on acetone powders and powders derived after drying indulin-acetone solution at 100 ^{o}C for 24 h.

For FTIR (Thermo Scientific Nicolet 8700 instrument), KBr and powders were mixed and then pressed into pellets. For each sample, a spectral range was collected from 400−4000 cm^{-1} after being scanned 32 times. Each pattern has a spectral resolution of 4 cm^{-1}. The peaks were then identified by using an analysis software (OMNIC 802, company, Thermo Fisher Scientific, Waltham, MA). TGA (TGA Q500, TA Instruments, 147 New Castle, DE) was performed at a heating rate of 10 °C/min until 950 °C in N_2 atmosphere. Differential Scanning Calorimetry (DSC Q1000, TA Instruments, New Castle, DE 19720) of CA-based blends were done from RT to 250 ^{o}C in N_2 environment. For all the other compositions, DSC were performed from RT to 200 ^{o}C in N_2 environment. In all cases, 20 ^{o}C/min heating rates were used.

2.2.6 Tensile Testing

Tensile testing was performed on the solvent casted samples by using a tensile testing machine (Shimadzu AD-IS UTM, Shimadzu Scientific Instruments Inc., Columbia, MD). Dog-bone shaped samples were cut from the solvent casted samples by using scissors according to dimensions listed in Figure 2.4. A total of 5 separate dog-bone samples were fabricated per lignin-bioplastic sample composition, for a total of 60 tensile samples. A deflection rate of 5 mm/min with a load cell of 5 kN was used to measure the stress vs displacement curve. For each sample,

the minimum width and thickness of the gauge area were measured using a Vernier caliper. These measurements were then used to measure the cross-sectional area for calculating the tensile stress during testing.

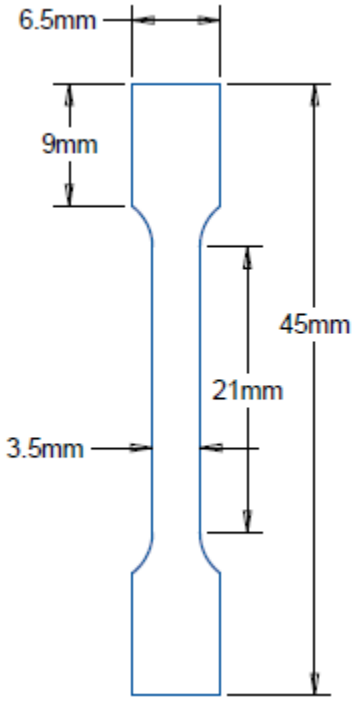

Figure 2.4: Schematics of dog-bone samples [17].

2.3 Results and Discussion

2.3.1 Solubility Studies

Figures 2.5 a and b show acetone-lignin solution after stirring in acetone for 2 and 24 h, respectively. The greater the solubility of lignin in acetone, the darker the solution become as higher amount of dark colored lignin was dissolved in the clear acetone solution. During experimentation, Dr. S. Gupta observed that lignin phase separated from acetone with the addition of water to the lignin-acetone solution. Figure 2.5c shows an example of phase separated lignin-water sol. On evaporation, lignin also deposits a coating on glass surfaces shown in Figure 2.5d. We will explore the design of nanoparticles and coating technology in the next chapters.

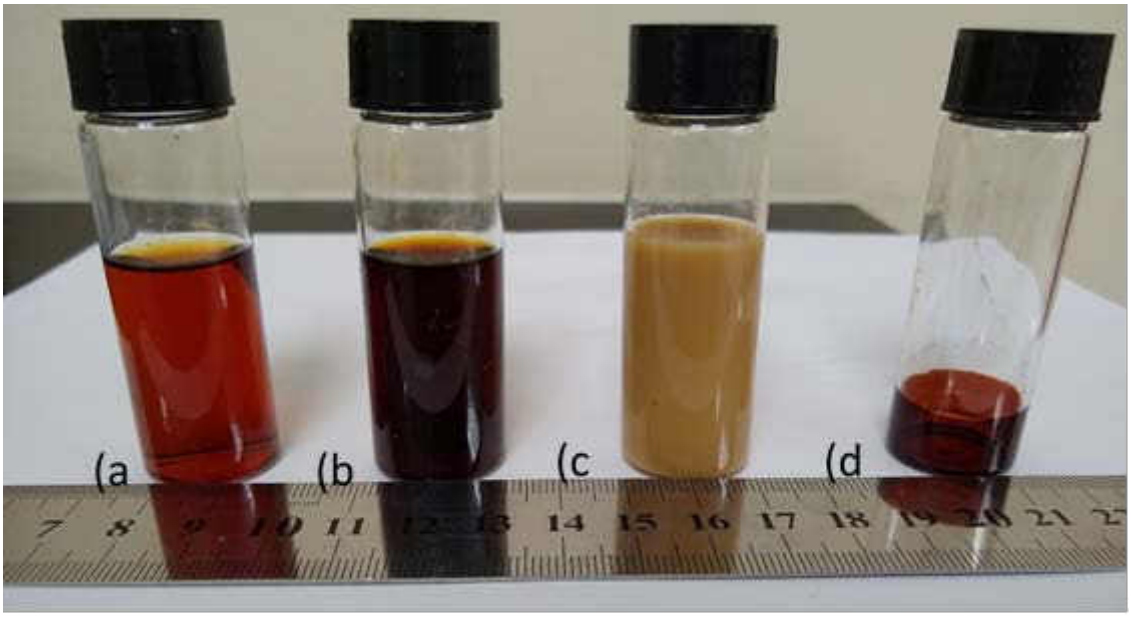

Figure 2.5: Lignin was partially dissolved in acetone after stirring for, (a) 2 h, (b) 24 h, (c) precipitation of nano-lignin by adding DI water, and (d) formation of lignin coating on glass surface after drying [picture courtesy: Dr. S. Gupta].

Figure 2.6 illustrates the solubility of lignin in acetone as a function of time. After stirring for 2 h, lignin (Sigma Aldrich) and indulin lignin had solubility of ~1.17 % and ~1.91%, respectively. After stirring for 24 h, the solubility of lignin (Sigma Aldrich) and indulin lignin increased to ~4.19% and ~3.72%, respectively as compared to ~4.89% and ~5.12% after 72 h of stirring. This shows that the solubility of lignin is slowing down after 24 h. For further research, we decided to use stirring for 24 h.

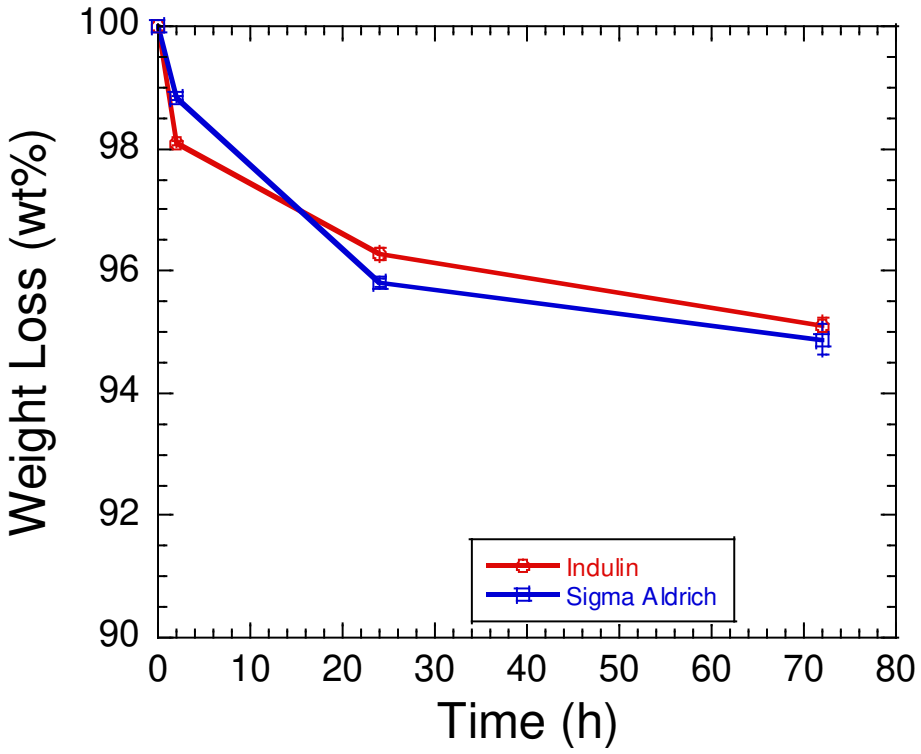

Figure 2.6: Solubility of lignin in acetone versus time.

2.3.2 FTIR, TGA, and DSC

Figures 2.7 a and b show the FTIR analysis of indulin lignin and acetone-lignin. Both indulin lignin and acetone-lignin showed similar behavior. Refer to reference [18] for the detailed identification of these peaks. Figure 2.7c shows the TGA of indulin lignin and acetone-lignin. Indulin lignin is more stable as compared to acetone-lignin. It is hypothesized that since acetone-lignin is extracted from indulin lignin, it has lower molecular weight as compared to indulin lignin hence it decomposes at lower temperatures. This hypothesis is further corroborated after the analysis of Figure 2.7d which shows acetone-lignin is decomposing at lower temperatures as compared to indulin lignin. Currently, we are measuring the molecular weight of acetone-lignin. These results will be published in follow up paper.

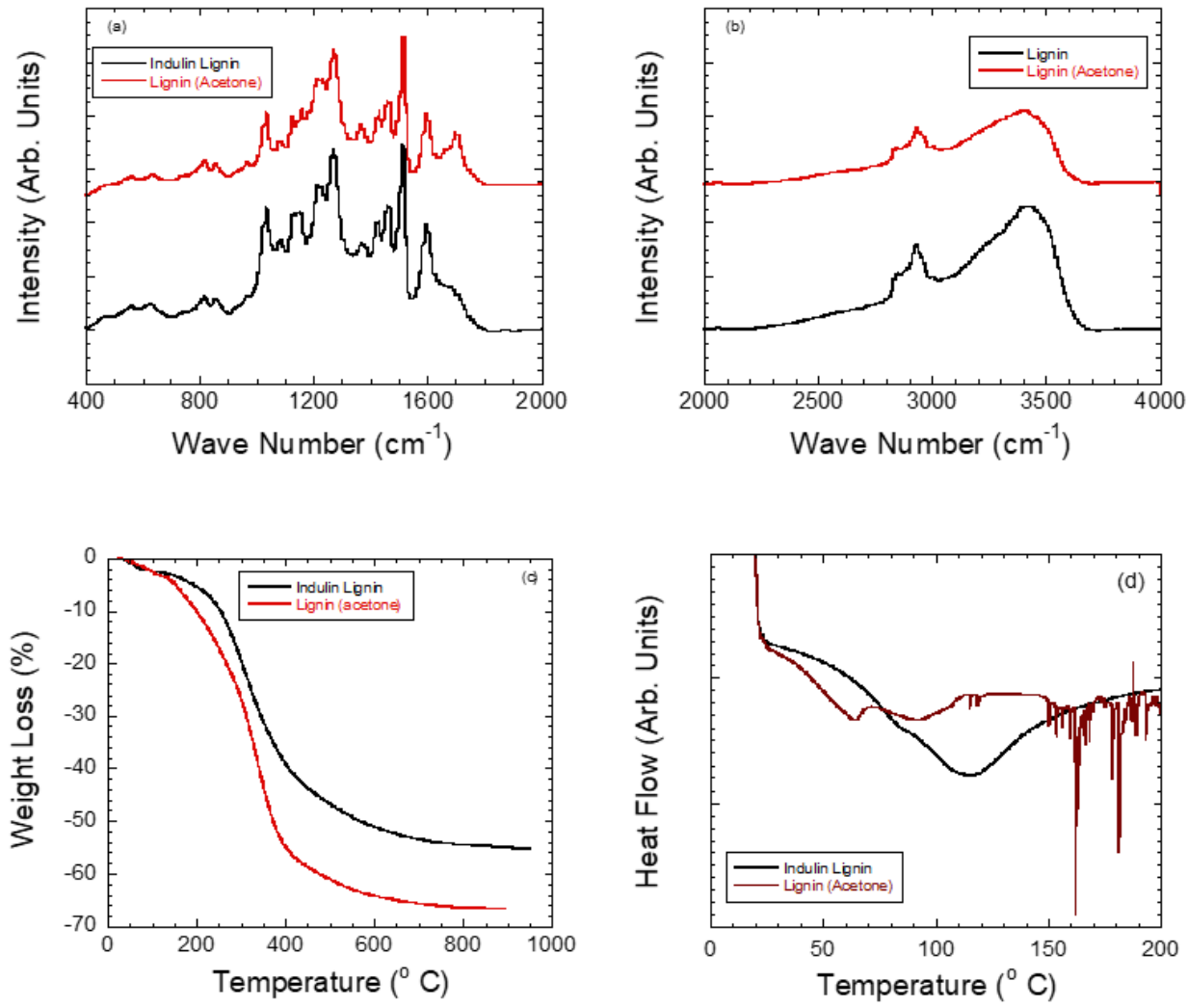

Figure 2.7: (a) FTIR (400-2000 cm^{-1}), (b) FTIR (2000-4000 cm^{-1}), (c) TGA, and (d) DSC analysis of indulin and lignin-acetone.

Figure 2.8 shows the DSC results of the various lignin bioplastic composites designed during this study. Figure 2.8a shows the comparison of CA, CA-3vol% lignin, and CA-9vol% lignin, respectively. CA is a predominantly amorphous polymer and demonstrates a glass transition temperature (T_g) at ~196 °C and a melting temperature (T_m) at ~230 °C. The addition of lignin enhances the amorphous nature of CA by lowering T_g to ~75 °C and ~145 °C, respectively. Since lignin does not melt, the lignin-CA composites undergo decomposition at around 200 °C, as seen by the instability in the data. This same instability occurs in lignin-acetone, as shown in Figure

2.7d. Based on these results, it is also hypothesized that phase separation between the lignin and CA is occurring.

Figure 2.8b shows the DSC plots of PLA, PLA-3vol% lignin, and PLA-9vol% lignin. PLA has T_g and T_m at ~62 and 149 °C, respectively. Comparatively, PLA-3vol% lignin also showed similar behavior. However, the addition of 9 vol% lignin reduced T_g and T_m to ~56 and ~144 °C, respectively. Figure 2.8c plots the comparison of PHA, PHA-3vol% lignin, and PHA-9vol% lignin, respectively. Pure PHA is semi-crystalline and has a crystallization temperature (T_c) at ~124 °C. PHA showed a melting point (T_{M2}) at ~150 °C and a minor melting peak (T_{M1}) was observed at ~60 ° C. This feature may be due to chain scission of PHA molecules [19]. The addition of lignin to PHA showed no or negligible T_c, and T_{M1} and T_{M2} decreased to ~54 and ~148 °C in PHA-9vol% lignin, respectively. Figure 2.8d shows the DSC plot of PLA-PHA, PLA-PHA-3vol% lignin, and PLA-PHA -9vol% lignin. The binary blend of PLA-PHA has a T_g, T_c, and T_m of ~61, ~130, and ~151 °C, respectively. PLA-PHA-3vol% lignin showed similar behavior as PLA-PHA blend. With the addition higher amount of lignin, T_g and T_m in PLA-PHA-9vol% lignin blend decreased to ~54 and ~148 °C, respectively.

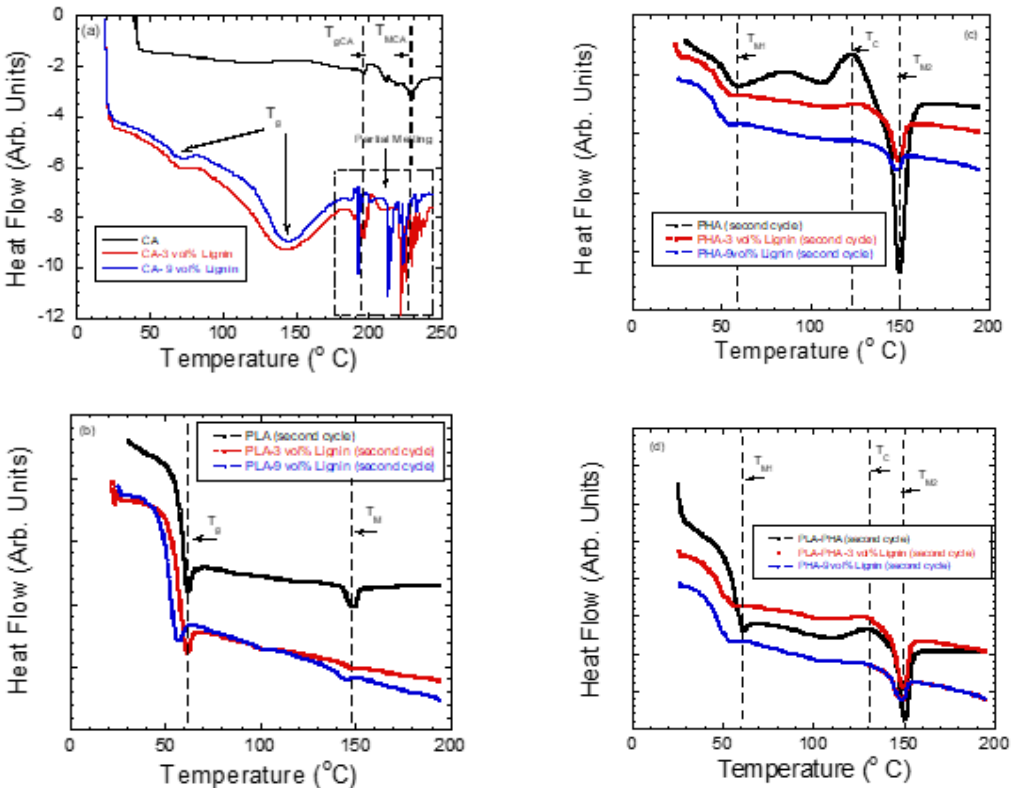

Figure 2.8: DSC plot of, (a) CA-lignin, (b) PLA-lignin (second heating cycle), (c) PHA-lignin (second heating cycle), (d) PLA-PHA-lignin (second heating cycle).

2.3.3 Tensile Strength

Figure 2.9a plots the tensile stress versus displacement behavior of CA, CA-3vol% lignin, and CA-9vol% lignin, respectively. The addition of lignin increased the tensile strength of CA matrix also shown in Figure 2.10. However, with the increased tensile strength, the composite became brittle as compared to pure CA.

Figure 2.9b shows the tensile stress versus displacement plot of PLA, PLA-3vol% lignin, and PLA-9vol% lignin, respectively. The addition of lignin in the PLA matrix decreased the UTS of PLA from ~59.4 MPa to ~34.3 MPa in PLA-9vol% lignin. Thus, the addition of lignin was found to degrade the mechanical properties of PLA like it was discussed in the introduction section.

Figure 2.9c shows the tensile stress versus displacement plot of PHA, PHA-3vol% lignin, and PHA-9vol% lignin, respectively. Unlike in the previous two bioplastics, the addition of lignin

in PHA increased the displacement at failure, meaning the addition of lignin made PHA more ductile. In addition, the UTS also increased slightly from ~17.4 MPa in PHA to ~18.7 MPa in PHA-9vol% lignin.

Figure 2.9d shows the tensile stress versus displacement plot of PLA-PHA, PLA-PHA-3vol% lignin, and PLA-PHA-9vol% lignin, respectively. As the percent volume of lignin is increased, the tensile strength is decreased from ~35.7 MPa in PLA-PHA to ~29.6 MPA in PLA-PHA-9vol% lignin. However, the displacement at failure increased which indicates that the samples are becoming more plastic with the addition of lignin. Earlier during DSC analysis, we had observed that the addition of lignin in PHA and PLA-PHA is acting like a plasticizer where it is decreasing the T_m of the blend. This may explain the enhanced ductility in these composites.

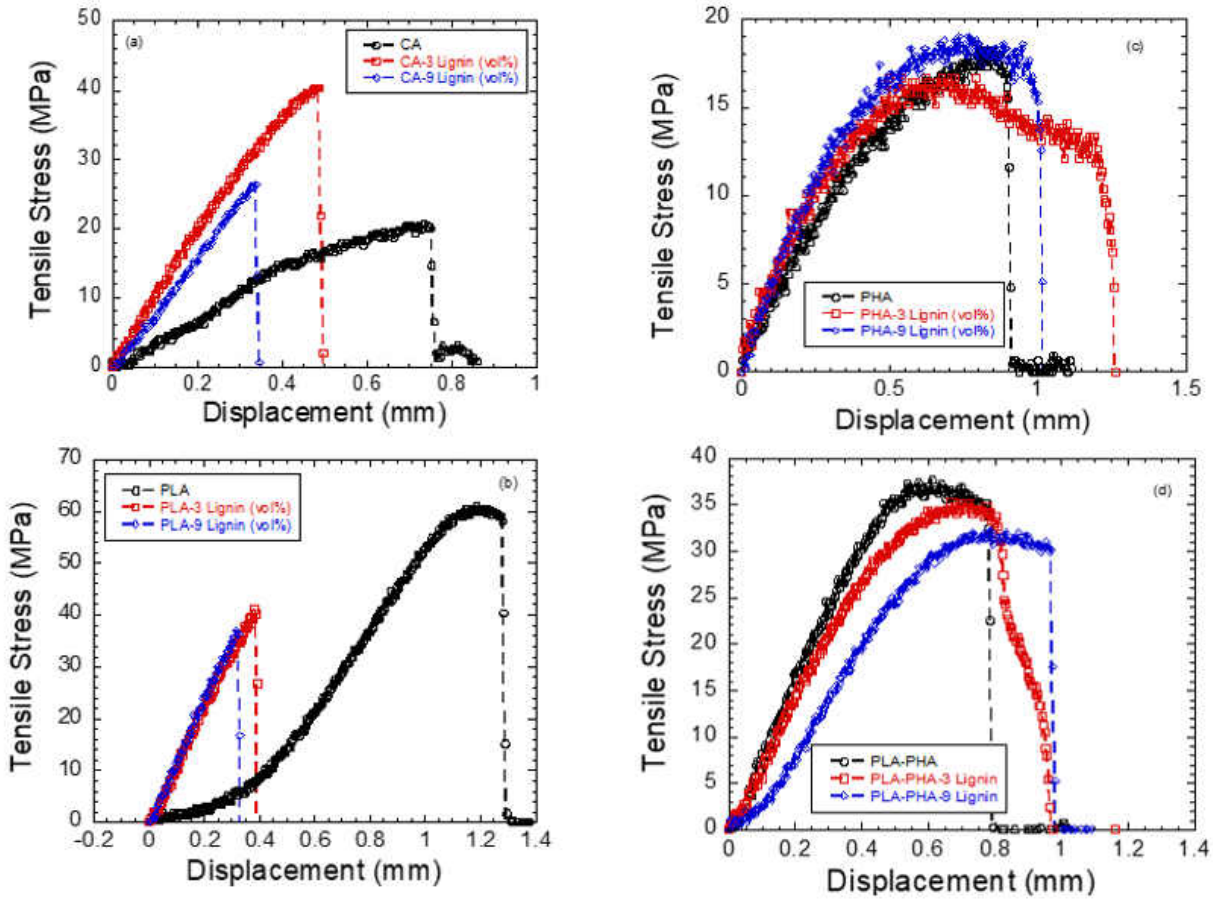

Figure 2.9: Plot of tensile stress versus displacement of (a) CA-lignin, (b) PLA-lignin, (c) PHA-lignin, and (d) 50%-50% PLA-PHA-lignin blends.

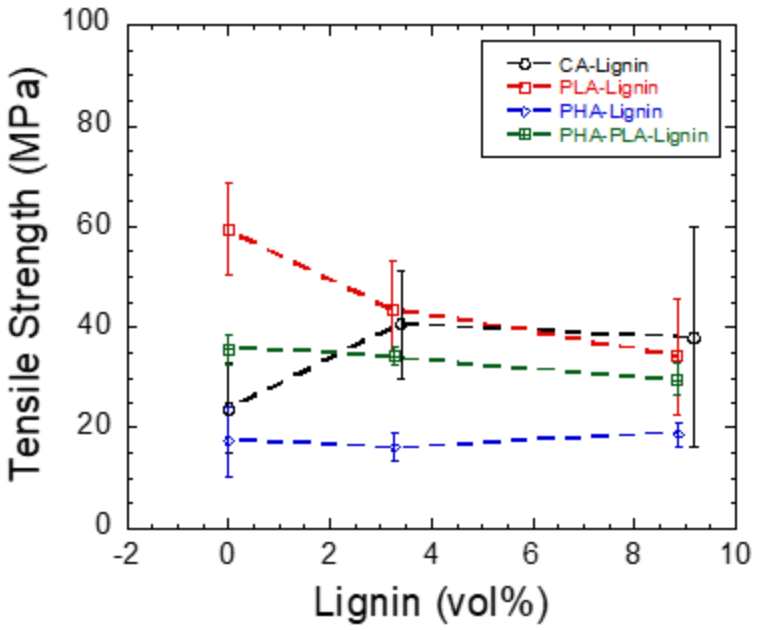

Figure 2.10: Plot of tensile strength of different blends as a function of lignin concentration.

Figures 2.11 a and b show the SEM images of fractured surface of CA-3vol% lignin at lower and higher magnification, respectively. Figure 2.11 c and d show SEM images of CA-9vol% lignin at a lower and higher magnification, respectively. On closer inspection of these images, we can observe heterogenous surface and pull-out in the fractured surface of CA-9vol% lignin as compared to CA-3vol% lignin. This further supports the fact that lignin and CA are demixing. Figures 2.11 e and f show SEM images of PLA-3vol% Lignin at a lower and higher magnification, respectively. Figures 2.11 g and h show SEM images of PLA-9vol% lignin in SE and BSE, respectively. On closer inspection, we can observe the phase separated spherical lignin particles on the fracture surfaces. This shows that the extent of phase separation in PLA-lignin is higher as compared to CA-lignin which is further reflected in the lower strengths of PLA-lignin blends as compared to CA-Lignin blends.

Figures 2.12 a and b show the SEM images of PHA-3vol% lignin at a lower and higher magnification, respectively. Figures 2.12 c and d show SEM images of PHA-9vol% lignin at a lower and higher magnification, respectively. Figures 2.12 e and f illustrate SEM images of a 50%-

50% PLA-PHA-3vol% lignin at both a lower and higher magnification, respectively. Figure 2.12 g and h depict SEM images of a 50%-50% PLA-PHA-9vol% lignin at both a lower and higher magnification, respectively. Overall, it can be observed in each case that the greater the amount of lignin added to the bioplastic matrix, the more heterogenous the fracture surface becomes. It appears that phase separation of lignin and bioplastic is occurring due to the contrast of the light areas found on the fracture surface with the dark areas. This suggests that a brittle fracture may be expected.

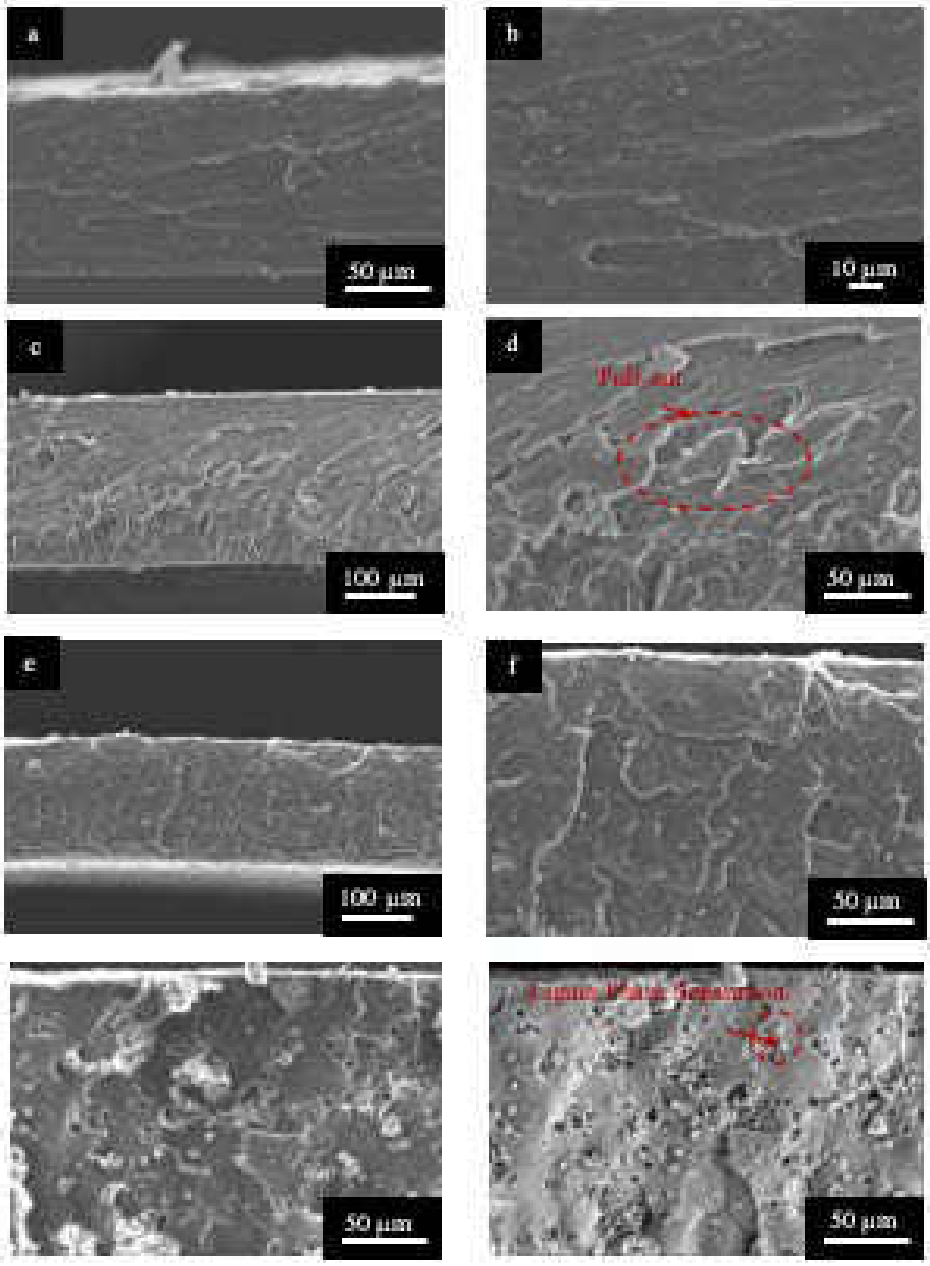

Figure 2.11: SE SEM micrographs of, (a) CA-3 vol% lignin, (b) CA-3 vol% lignin (higher magnification), (c) CA-9 vol% lignin, (d) CA-9 vol% lignin (higher magnification), (e) PLA-3 vol% lignin, (f) PLA-3 vol% lignin (higher magnification), (g) PLA-9 vol% lignin, (f) PLA-9 vol% lignin in BSE.

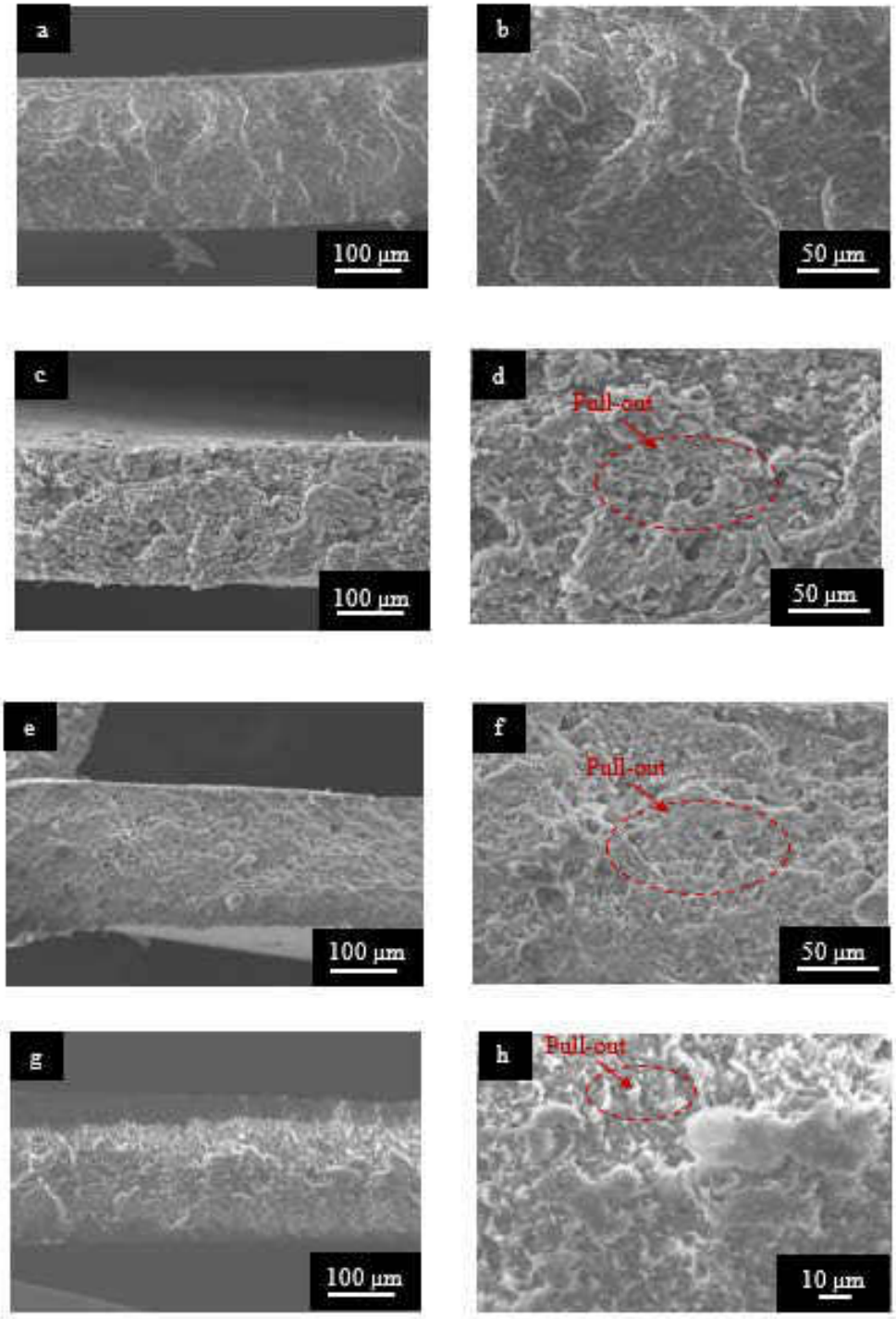

Figure 2.12: SEM micrographs of, (a) PHA-3 vol% lignin, (b) PHA-3 vol% lignin (higher magnification), (c) PHA-9 vol% lignin, (d) PHA-9 vol% lignin (higher magnification), (e) PLA-PHA-3 vol% lignin, and (f) PLA-PHA-3 vol% lignin (higher magnification), (g) PLA-PHA-9 vol% lignin, and (h) PLA-PHA-9 vol% lignin (higher magnification).

2.4 Conclusions

We have developed a procedure for designing lignin-acetone solution by using a benign extractive process. FTIR analysis indicates that indulin lignin and acetone-lignin have similar chemical structure. Dr. S. Gupta's group is performing further in-depth studies to understand the molecular structure of acetone-lignin by performing molecular weight analysis. TGA analysis showed that acetone-lignin is less stable at higher temperatures than indulin lignin powders. Detailed microstructure and mechanical behavior study of lignin reinforced biocomposites were performed during this study.

CHAPTER III: DESIGN AND CHARACTERIZATION OF LNP FROM LIGNIN-WATER SOL

3.1 Introduction

There are a variety of methodologies to manufacture LNPs. In the introduction section, we have outlined different procedures for fabricating LNPs. In this chapter, acetone-lignin is made into a lignin-water sol to design LNPs by using a relatively simple water dilution process.

3.2 Experimental Details

3.2.1 Manufacturing Process

Lignin-acetone solution was fabricated by using the procedure described in the last chapter. Table 3.1 summarizes different lignin-acetone stock solution. Lignin nanoparticles were precipitated by adding a controlled amount of water in the lignin-acetone shown in Table 3.2. Figure 3.1 illustrates the experimental procedure for creating lignin-water sol. The compositions referred to as batch-1 were used for particle size measurements. The compositions referred to as batch-2 were used for zeta potential and microscopy measurements. For determining the density of acetone-lignin, HTS5-27-1 was dried at 100 ºC for 24 h. Thereafter, the powder was crushed and sieved by -325 mesh slides. During this process, -325 mesh powders were collected for further analysis. For volumetric calculations, the density of acetone-lignin was performed by He pycnometer Ultrapyc 1200e (Quantochrome Instruments, 212 Boynton Beach, Florida).

Table 3.1: Composition of lignin-acetone solution

Sample Code	Composition	Lignin (wt%)
LN1-2-3	Acetone-Lignin- (Batch-1)	3.48±0.23
HTS5-27-1	Acetone-Lignin- (Batch-2)	4.63±0.12
HTS5-19-10	Acetone-Lignin-1 wt% (Batch-1)	~1 wt%
HTS5-19-11	Acetone-Lignin-0.5 wt% (Batch-1)	~0.5 wt%
HTS5-19-12	Acetone-Lignin-0.1 wt% (Batch-1)	~0.1 wt%
HTS5-28-4	Acetone-Lignin-1 wt% (Batch-2)	~1 wt%
HTS5-28-5	Acetone-Lignin-0.5 wt% (Batch-2)	~0.5 wt%
HTS5-28-6	Acetone-Lignin-0.1 wt% (Batch-2)	~0.1 wt%

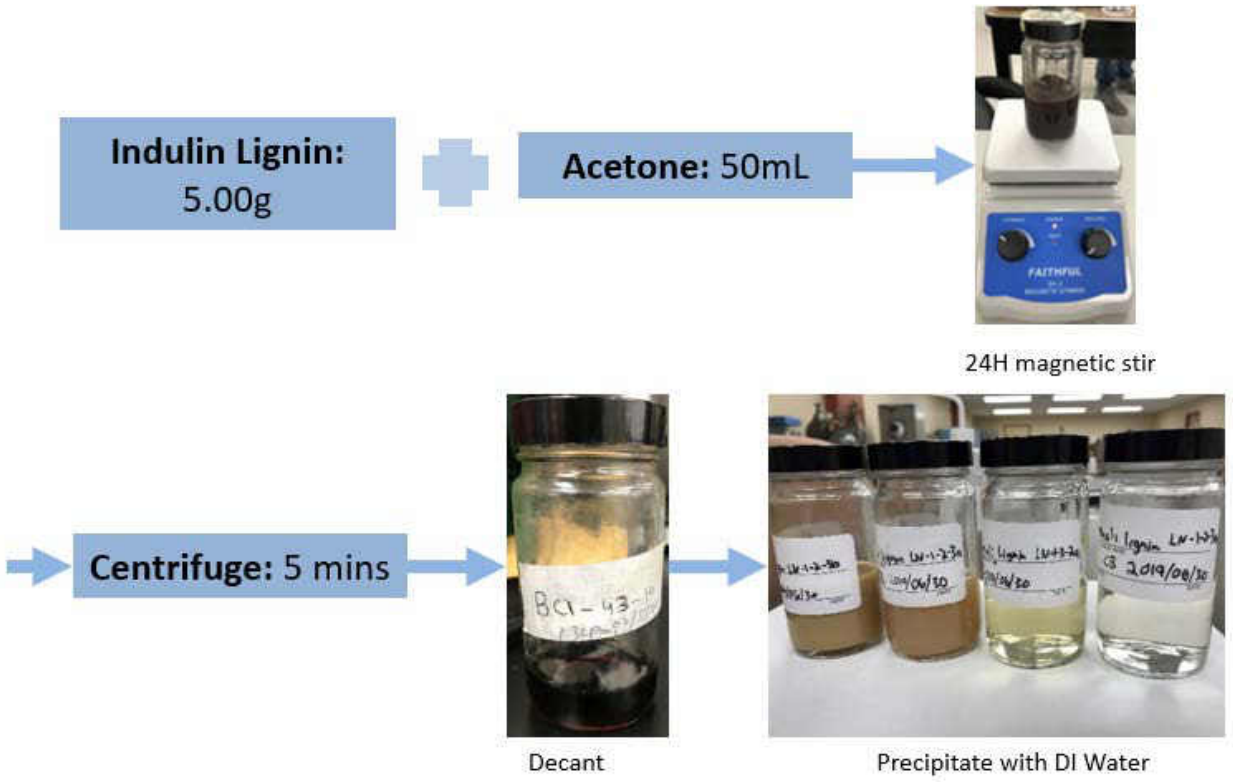

Figure 3.1: Procedure to create lignin-water sol.

3.2.2 Particle Size Characterization

Nicomp 380 (Particle Sizing Systems, Port Richey, FL) was used for particle size analysis. A critical condition for using this instrument is that the intensity of signal should be less than 250 KHz. Due to this limitation, concentrated lignin-water solution cannot be measured by using this method. In all the experiments, Chi was less than 3, thus we used Gaussian fitting to interpret the results. In DLS, three gaussian curves are given for each particle size measurement which each present a mathematical approach to estimating the average particle size. The first of the approaches is number average weighting which is proportional to the first power of the particle size. The second approach is volume average weighting which is proportional to the third power of the particle size. The third and final approach is scattering intensity weighting which is proportional to the sixth power of particle size. In general, number average weighting estimates the average

particle size to be the smallest of the three approaches while scattering intensity estimates the average particle size to be the largest. For the sake of consistency, the volume average distribution has been chosen to report the average particle size of the lignin-water sol samples [20].

3.2.3 Zeta Potential Characterization

Zetasizer Nano ZS (Malvern, Worcestershire, UK) was used to measure zeta potential. These experiments were conducted by Mr. D. Sun from the Department of Chemistry, University of North Dakota. During testing, disposable folded capillary cells, DTS1070, were used at 25.0 °C. For each experiment, equilibration time was set to 120 s and the measurement angle was set to 173˚ Backscatter (NIBS default) under automatic control. For each sample, three measurements were performed.

Table 3.2 shows the compositions used for measurements. These samples were then utilized for zeta potential characterization, as well as mobility and conductivity measurements.

Table 3.2: Volume percentage of lignin in a lignin-water sol for each sample

Sample Code	Stock Solution	DI water (ml)	Lignin (vol%)
HTS5-29-1	HTS5-27-1 (0.5 ml)	50	0.03
HTS5-29-2	HTS5-28-4 (0.5 ml)	50	0.006
HTS5-29-3	HTS5-28-5 (1.2 ml)	40	0.009
HTS5-29-4	HTS5-28-6 (1.2 ml)	40	0.002
HTS5-29-5	HTS5-28-5 (1 ml)	10	0.03
HTS5-29-6	HTS5-28-6 (1 ml)	10	0.24

3.2.4 SEM Analysis of Nanoparticles

An aluminum stud (Product ID 16231, Ted Pella Inc., Redding, CA) was polished until 1 μm finishing; thereafter, 100 μL of lignin-water sol from the various samples listed in Table 3.2 were dropped onto the polished sample. Finally, the aluminum stud was placed into an oven at 100 °C and dried for 24 h.

3.2.5 ImageJ Analysis of SEM Characterization

A scanning electron microscope (SEM, JEOL JSM-6490LV, JEOL USA, Inc., Peabody, Massachusetts) in secondary electron (SE) mode was used to document the dried samples. For further understanding of the particle size, a total of 10 randomly distributed particles were analyzed in an SEM micrograph with a total of 3 measurements per particle measured by using a NIH software. Both the average particle size and standard deviation are reported.

3.3 Results and Discussion

3.3.1 DLS

Figure 3.2 shows the particle size distribution of different sols. Table 3.3 shows the summary of reading. In general, we were successful in designing lignin-particles in the range of 58-33 nm. In addition, we also observed that the greater the dilution of lignin in water, the smaller the lignin nanoparticles become. It is believed the mechanism that causes this is agglomeration between the lignin nanoparticles. We will discuss it in detail in the next section.

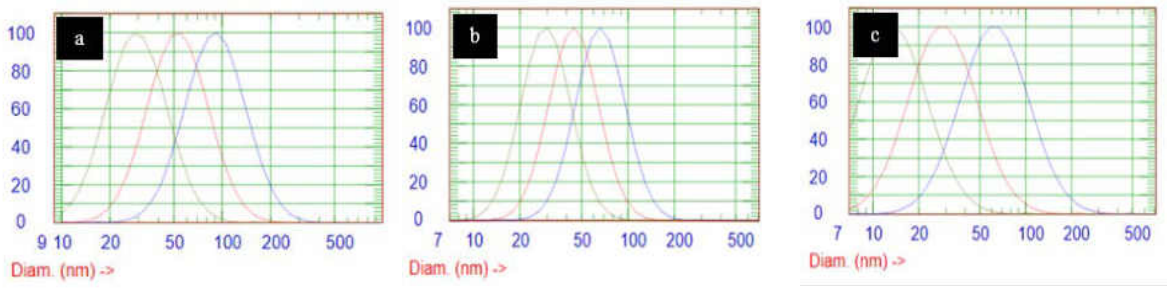

Figure 3.2: Plot of intensity versus particle size of, (a) HTS5-19-10 (water), (b) HTS5-19-11 (water), and (c) HTS5-19-12 (water).

Table 3.3: Particle size of lignin in a lignin-water sol

Composition	Lignin (vol%)	Particle Size (nm) [vol distribution]
HTS5-19-10 (40 µl)-water (4 ml)	0.006	58 ± 25
HTS5-19-11 (40 µl)-water (4 ml)	0.003	48 ± 18
HTS5-19-12(120 µl)-water (4 ml)	0.002	33 ± 17

3.3.2 Zeta Potential, Mobility, and Conductivity

The results of zeta potential analysis measured for various lignin concentrations may be found in Figure 3.3 a and d. Figure 3.3a shows lignin for different concentrations is mildly stable. According to Joseph et al. [21], zeta potential stability is reached at a value equal to or greater than ± 30mV [21]. Some of the concentrations are seen to be above this threshold such as 0.03 vol% lignin, while some concentrations are below the 30mV stability threshold like 0.24 vol% lignin. An additional observation is that after 7 days and 14 days, the stability tends to remain at similar values. This indicates that the lignin-water sol has longer-term storage stability and has potential to be sold as a product. In Figure 3.3d, the same measurements were taken only at an elevated temperature of 70 °C for 10 minutes, above the boiling point of acetone. Earlier, it was assumed that the volume of acetone in the lignin-water sol would be low enough to ignore. The zeta potential

values of the lignin-water sol after heating to ensure the acetone was vaporized out of the water are very similar to Figure 3.3a. Thus, it is believed the presence of a small amount of acetone in the lignin-water sol does not impact the stability.

In Figure 3.3b the results of mobility as a function of lignin concentration are shown. Since the mobility values are found to be all negative, it can be assumed that the lignin-water sol is consistently negatively charged in all concentrations. In Figure 3.3c the results of conductivity as a function of lignin concentration are depicted. In general, the higher the lignin concentration is, the greater the conductivity.

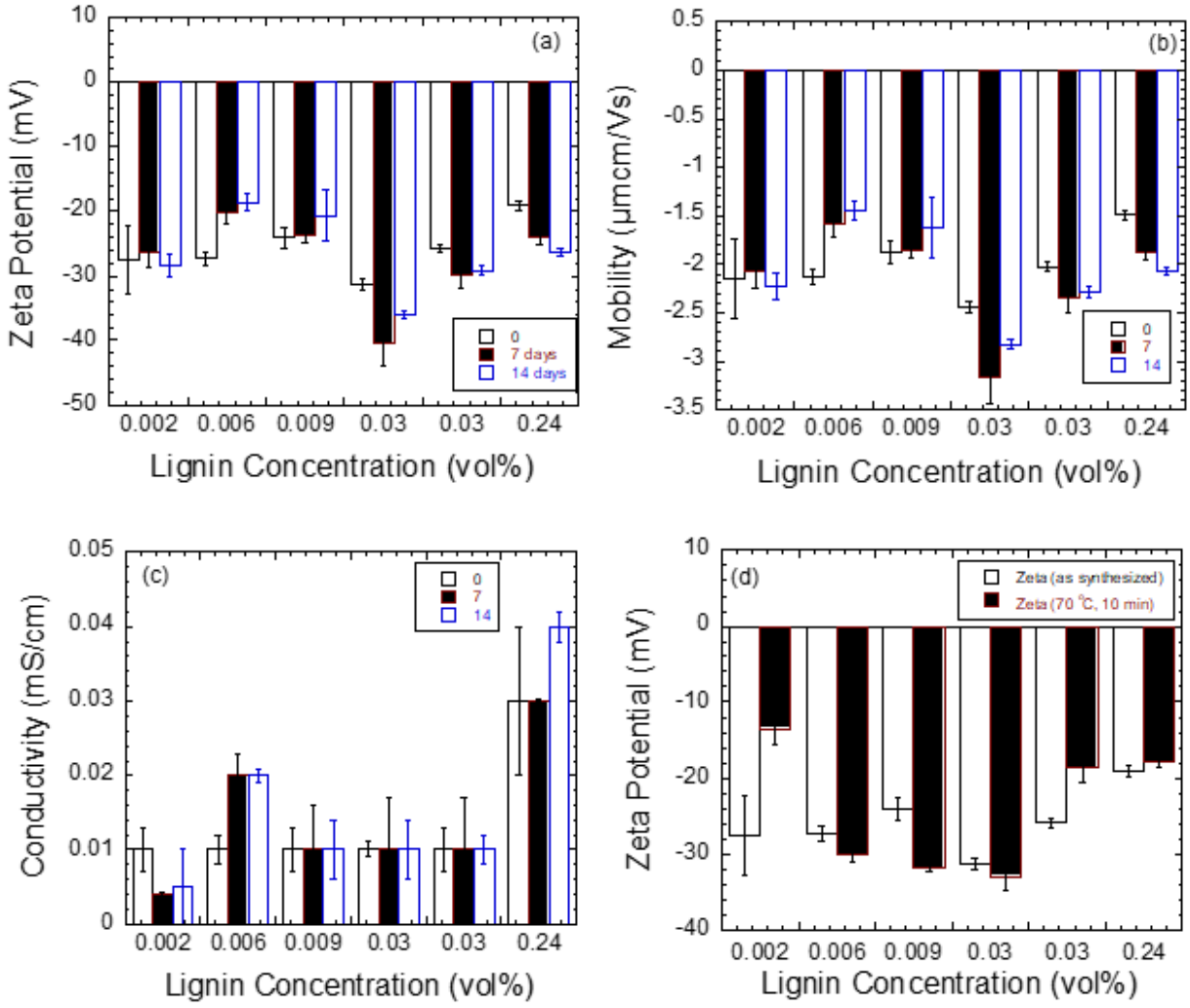

Figure 3.3: Plot of, (a) zeta potential, (b) mobility, (c) conductivity, and (d) zeta potential (stability) as a function of lignin concentration in the solution.

3.3.3 SEM Analysis of Nanoparticles

SEM images were taken of each aluminum stud that had lignin-water sol of various lignin concentrations dropped on it. The SEM images at two different magnifications for each sample are shown below in Figure 3.4. The results of ImageJ are shown in Table 3.4. From this data, a lignin particle size of 200, 205, and 192 nm was found for samples with a vol% lignin of 0.03, 0.006, and 0.009, respectively. The smallest average particle size measured with ImageJ was 150 nm found on one of the samples with a vol% lignin of 0.03. Another observation is that the sample with the

highest vol% lignin of 0.24 had inconclusive lignin particle size. It is believed that the lignin in water agglomerated, forming visible flakes as seen in Figure 3.4 k and l. Finally, the sample with the lowest concentration of lignin had a vol% lignin of 0.002 had the largest average particle size measurement of 652 nm. It is believed that since this solution was so diluted, the SEM analysis was challenged trying to picture enough lignin nanoparticles.

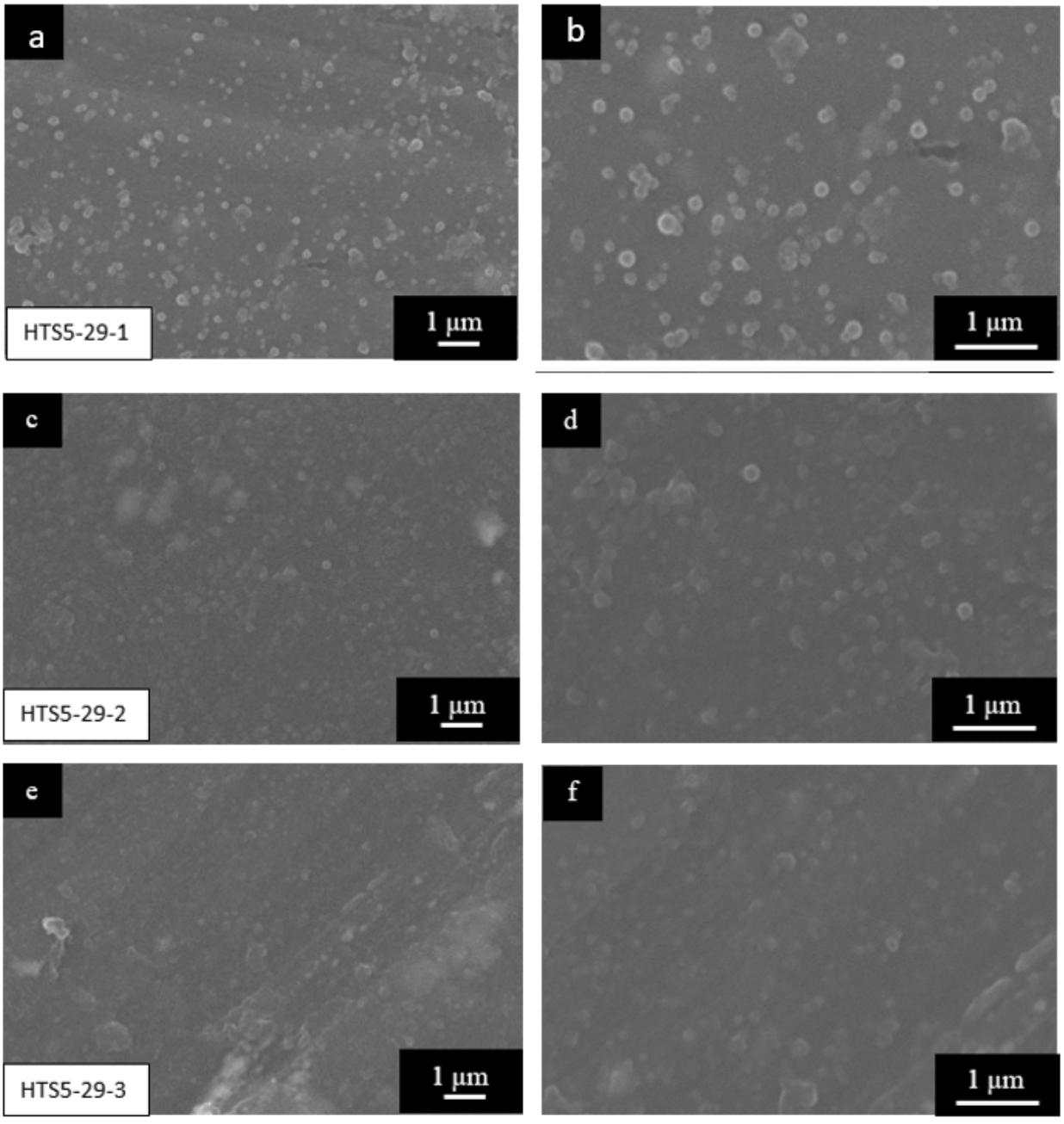

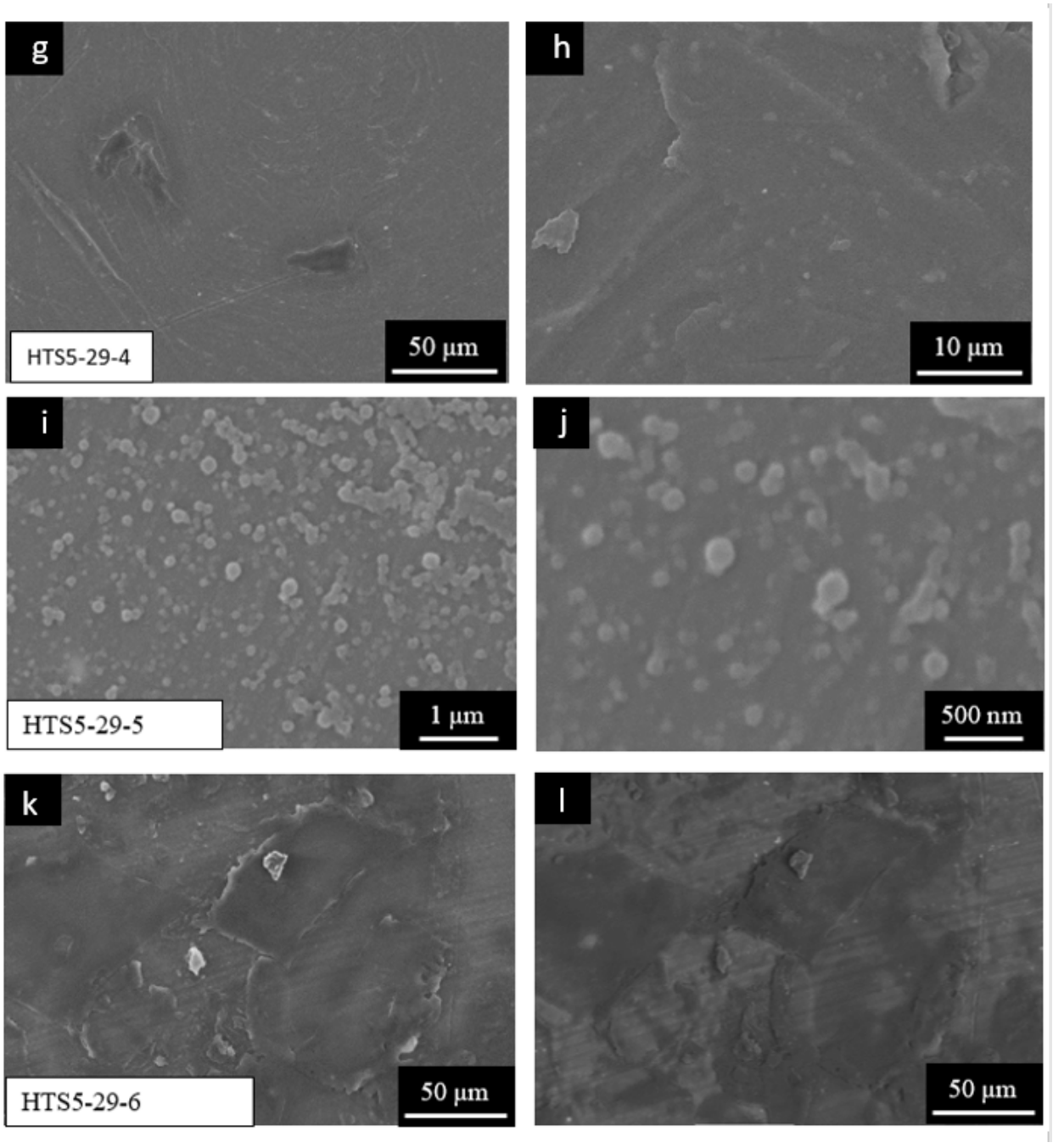

Figure 3.4: SEM of, (a) HTS5-29-1, (b) HTS5-29-1 (higher magnification), (c) HTS5-29-2, (d) HTS5-29-2 (higher magnification), (e) HTS5-29-3, (f) HTS5-29-3 (higher magnification), (g) HTS5-29-4, (h) HTS5-29-4 (higher magnification), (i) HTS5-29-5, (j) HTS5-29-5 (higher magnification), (k) HTS5-29-6, and (l) HTS5-29-6 (higher magnification).

Table 3.4: Particle size of LNP on Al stud measured using ImageJ analysis of SEM

Sample	Particle size (um)	Standard deviation (um)	# Particles analyzed	# Measurements per particle	Lignin (vol%)
HTS5-29-1	0.200	0.031	10	3	0.03
HTS5-29-2	0.205	0.027	10	3	0.006
HTS5-29-3	0.192	0.035	10	3	0.009
HTS5-29-4	0.652	0.258	10	3	0.002
HTS5-29-5	0.150	0.032	10	3	0.03
HTS5-29-6	N/A	N/A	N/A	N/A	0.24

3.4 Conclusions

The addition of water to a lignin-acetone solution precipitates the lignin out of the acetone and forms nano sized particles when diluted enough. Particle sizes of the lignin-water sol were measured by DLS and found to be as small as 33 nm based on the average volume weighting. Zeta potential analysis concluded that lignin-water sol is mildly stable, has potential to be stable over time, and the stability is not impacted by the presence of acetone in the lignin-water sol. Solid lignin nanoparticles may be produced by depositing a highly diluted lignin-water sol onto a polished substrate surface. Particle sizes of around 200 nm have been reported, with the smallest particle size being 150 nm.

CHAPTER IV: DESIGN AND CHARACTERIZATION OF LIGNIN COATINGS

4.1 Introduction

The inspiration for pursuing coatings as a potential application of lignin and LNPs began during the solubility study in the preceding chapters. A thin, complete coating was observed after the drying stage of lignin-acetone in a glass container.

In this experiment, a drip coating is applied to three different substrates. Depending on the substrate used in drip coating, a surface may act as hydrophilic, water loving, or hydrophobic, water fearing. One key factor to pay close attention to is the surface and its preparation. Hydrophobicity relies heavily on the tribological properties of a material. In addition, at the nanoscale, surface properties typically dominate material properties over the bulk constituent.

4.2 Experimental Design

4.2.1 Manufacturing Process

To begin the experiment, three different substrates were gathered including: stainless steel, mica (Highest Quality Grade V1 mica, MTI Corporation, Richmond, CA), and Corning glass (Corning EAGLE XG Glass Substrates, MTI Corporation, Richmond, CA). These three substrates were used for their relatively fine surface finishes as well as to provide a variety substrate material. A glass pipet was used to deposit 250 μL of 4.6% wt. lignin dissolved in acetone (Composition HTS5-27-1, Chapter 3). Once the lignin-acetone solution has been dropped onto each substrate, the samples were dried completely at 100 ^{o}C for 24 h.

Digital photos were taken of the stainless steel, mica, and Corning glass substrates along with the lignin dissolved in acetone coated substrates (Figure 4.1). Figures 4.1 a and b depict lignin-acetone coated stainless-steel and a stainless-steel substrate, respectively. Figure 4.1 c and d illustrate lignin-acetone coated mica and an as-received mica substrate, respectively. Finally,

Figure 4.1 e and f show the lignin-acetone coated Corning glass and as-received Corning glass, respectively.

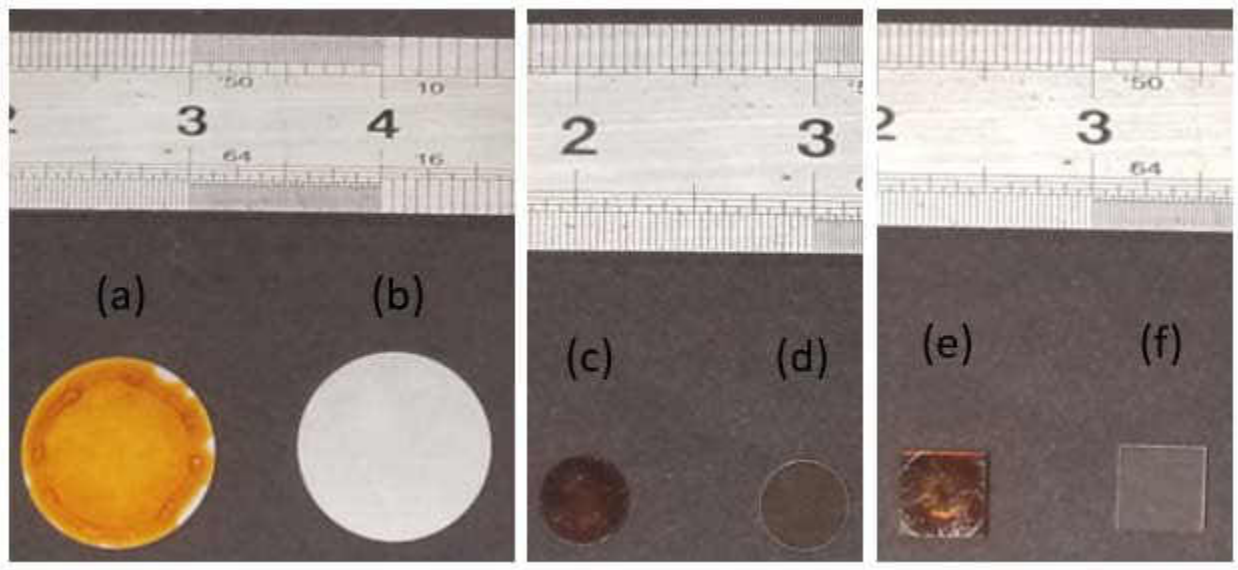

Figure 4.1: (a) lignin-acetone coated stainless-steel, (b) stainless-steel, (c) lignin-acetone coated mica, (d) as-received mica, (e) lignin-acetone coated Corning glass, and (f) as-received Corning glass.

4.2.2 Optical Microscopy, SEM, Wettability, and Vickers Hardness Characterization

To visually analyze the lignin coatings which formed on substrates, optical microscopy at 10X magnification was performed as well as SEM imaging of the coatings. Next, wettability was performed on each substrate and compared to the lignin coated substrate. Materials behave hydrophobically if the contact angle with water is greater than 90° and hydrophilic if the contact angle is less than 90°. Finally, Vickers hardness testing was performed to verify the performance of the lignin coating on each substrate. The load was set to 0.3 kg for a time duration of 15 seconds.

4.3 Results and Discussion

4.3.1 Optical Microscopy

The optical microscopy can be seen below in Figure 4.2. Figure 4.2 a and b depict the as-received mica and acetone-lignin coated mica substrate, respectively. Figure 4.2 c and d depict as-

received Corning glass and acetone-lignin coated Corning glass, respectively. Figure 4.2 e and f depicts as received stainless-steel and acetone-lignin coated stainless-steel sample, respectively. In each case, lignin evenly and sufficiently covered each substrate.

Figure 4.2: Optical microscopy at 10X magnification of (a) as-received mica, and (b) lignin-acetone coated mica (c) as-received Corning glass, (d) lignin-acetone coated Corning glass, (e) as received stainless-steel, and (f) lignin-acetone coated stainless-steel.

4.3.2 SEM

The SEM images of lignin, various substrates, and their lignin coated counterparts are shown in Figure 4.3. Figures 4.3 a and b show two different magnification levels of dried and

crushed lignin after being dissolved in acetone. The lignin particles seen are of various shapes due to the milling process. Figures 4.3 c and d illustrate SEM micrographs of the as received mica substrate and mica substrate after being coated with lignin dissolved in acetone-lignin, respectively. Figure 4.3 e and f show the SEM micrographs of stainless-steel as received and after coating with acetone-lignin, respectively. It can be noticed that the grooves from the previous surface finish can no longer be seen on the stainless-steel substrate which indicates uniform distribution of the coating. Figure 4.3 g and h show the SEM micrographs of Corning glass substrate as received and Corning glass micrograph after the addition of lignin dissolved in acetone, respectively. There appears to be both a fine coating of lignin on the substrate as well as agglomeration of lignin on the substrate.

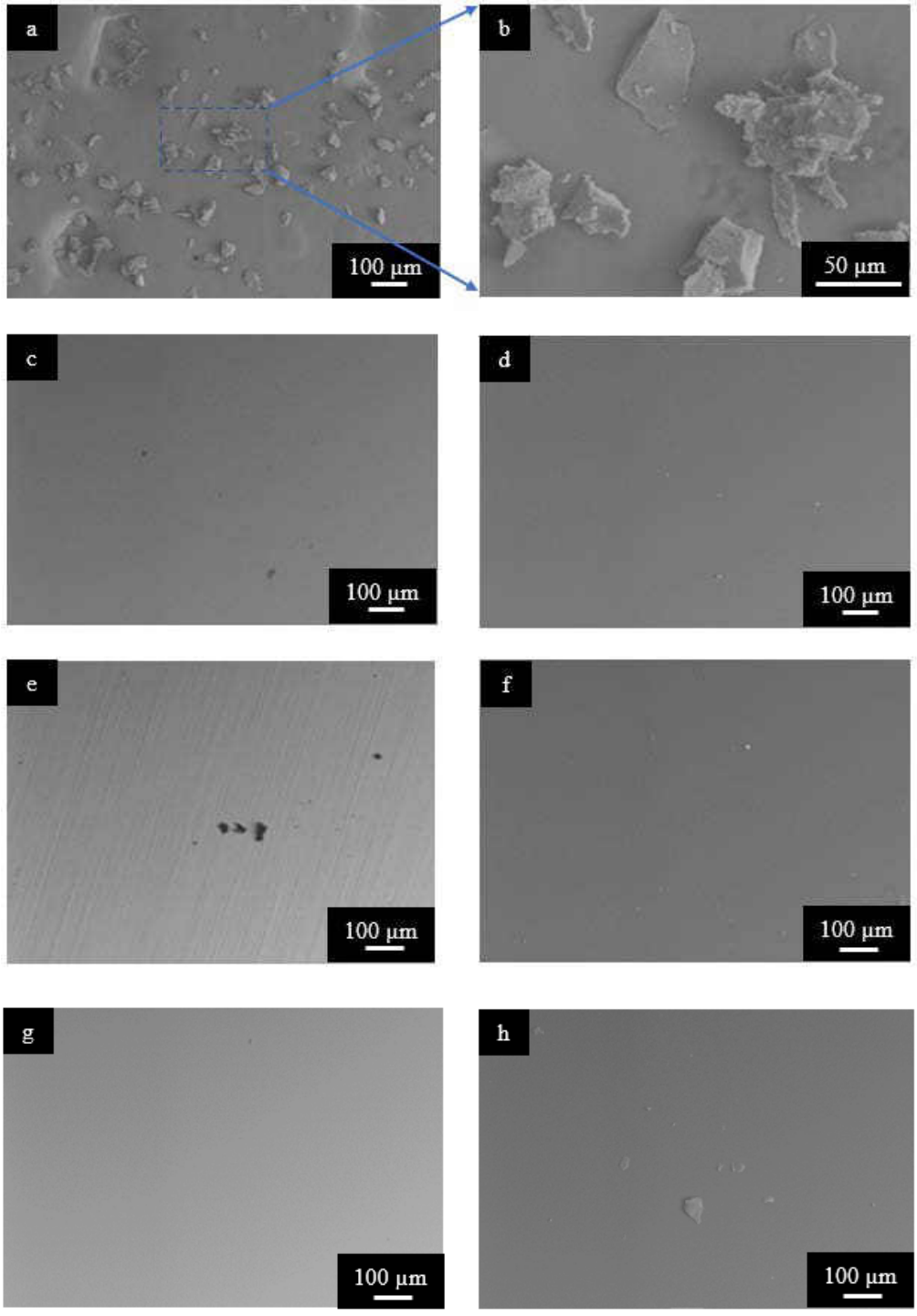

Figure 4.3: SEM micrographs of, (a) dried and crushed lignin-acetone, (b) dried and crushed lignin-acetone at higher magnification, (c) as-received mica, (d) lignin-acetone coated mica, (e) as-received stainless-steel, (f) lignin-acetone coated stainless-steel, (g) as-received Corning glass, and (h) lignin-acetone coated Corning glass.

4.3.3 Wettability

Wettability analysis was also performed on the lignin coated substrates. Figures 4.4 a, b, and c depict the results of a water droplet on mica, Corning glass, and stainless-steel, respectively. The wettability results of a water dropplet on the mica, Corning glass, and stainless-steel substrates coated with acetone-lignin can be seen in Figure 4.4 d, e, and f, respectively. In all cases, the experiment resulted in the substrates being hydrophilic because the angle for each measurment was found to be below 90 degrees. The acetone-lignin coated mica and Corning glass were more hydrophobic as compared to pristine samples while the acetone-lignin coated stainless-steel composition was more hydrophilic. It is interesting to note that the lignin coating performed with a similar wettability in all three cases, indicating that a lignin coating may be used to tailor the wettability of various substrates.

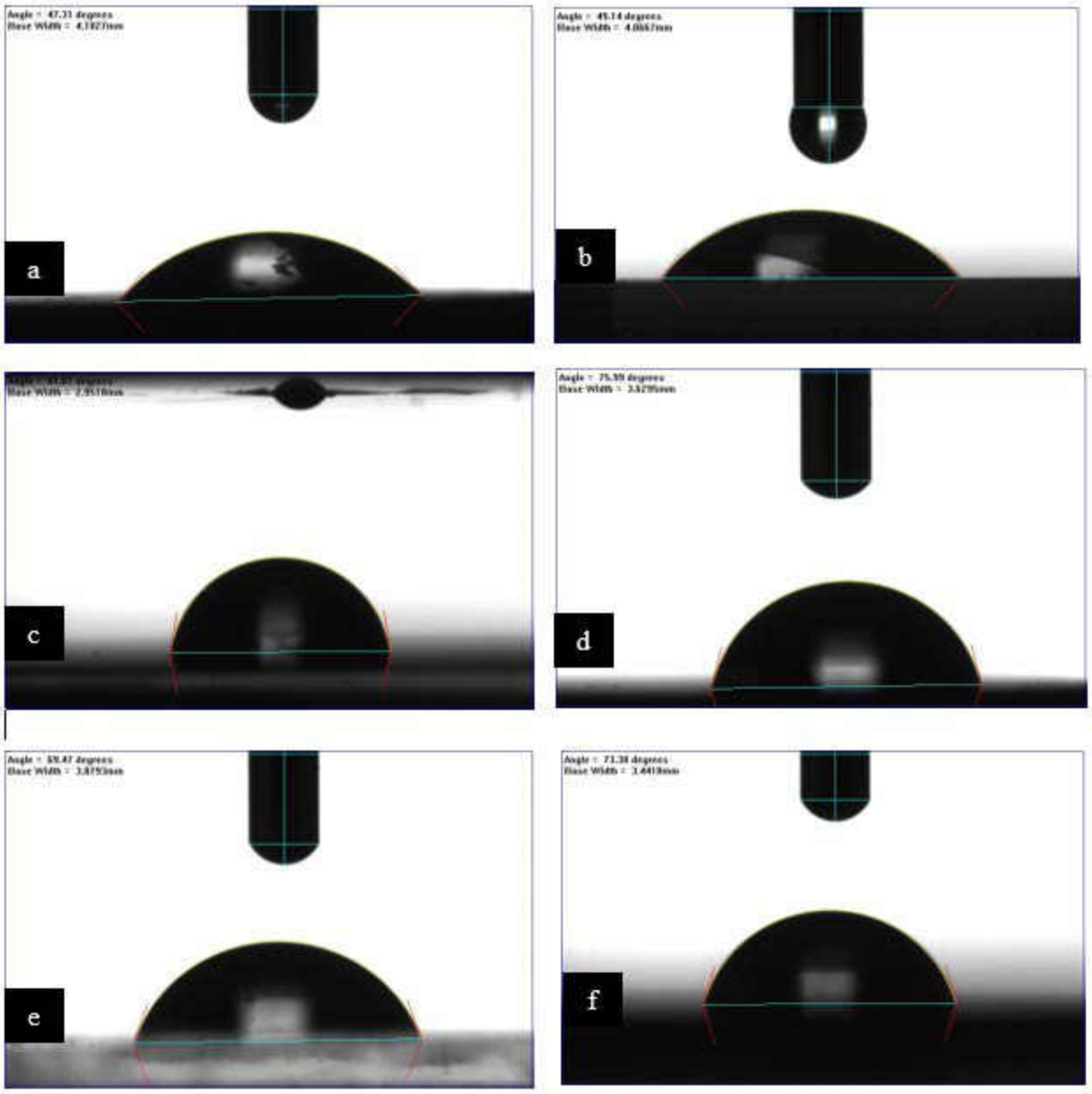

Figure 4.4: Water droplet on as-received, (a) mica, (b) Corning glass, and (c) stainless steel, and lignin-acetone coated surface of, (d) mica, (e) Corning glass, and (f) stainless steel.

4.3.4 Vickers Hardness

Vickers hardness testing was performed on each of the three substrates and their lignin coated counterparts as shown in Figure 4.5. In the case of stainless-steel and mica, the lignin coating showed cracking and pealing (Figs. 4.5 b, c). However, the Corning glass substrate showed no cracking of the lignin coating, indicating a more stable lignin coating (Figs.4.5 h, i) as compared

to acetone-lignin coating on mica which showed intermediate behavior were some signs of crack was observed (Figs. 4.5 e, f).

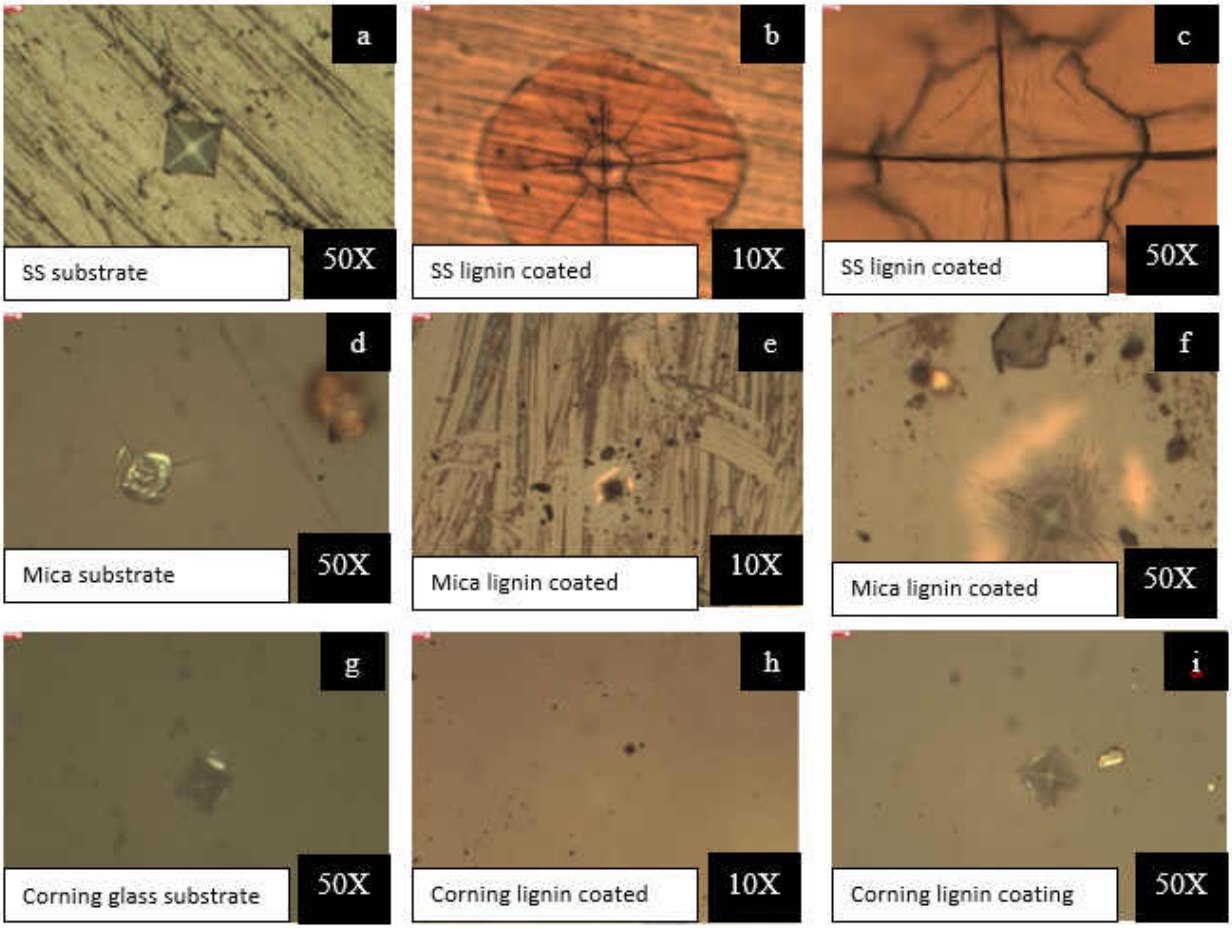

Figure 4.5: Optical microscopy of Vickers hardness indentation with a 0.3 kg load for 15 seconds of (a) stainless-steel at 50X, (b) stainless-steel lignin coated at 10X, (c) stainless-steel lignin coated at 50X, (d) mica substrate at 50X, (e) mica lignin coated at 10X, (f) mica lignin coated at 50X, (g) Corning glass substrate at 50X, (h) Corning lignin coated at 10X, and (i) Corning lignin coated at 50X.

4.4 Conclusions

Lignin-acetone solution may be utilized to form coatings on various substrates, including forming a stable coating on Corning glass based on Vickers hardness results. Lignin coatings may be used to help tailor a substrates wettability to either more hydrophobic or hydrophilic, depending on the wettability of the original material.

CHAPTER V: DESIGN OF ULTRASONIC SPRAY SET UP AND FUTURE WORK

5.1 Introduction

In this chapter, a process to coat materials with lignin nanoparticles was developed using an ultrasonic sprayer. The aim was to coat substrates while preventing the agglomeration of LNPs, as seen in the drip coating experiment. Potential applications include tailor-made nano-coatings on various substrates or materials. To achieve this goal, an ultrasonic spray was used to deposit LNPs on a substrate.

5.2 Experimental Design

5.2.1 Manufacturing Process

An ultrasonic power supply was connected to a sonicator with an atomizer nozzle as seen in Figure 5.1. The ultrasonic power supply had to be connected to a transformer to turn the U.S. 110V into 220V output. On a scale of 1-3, an output of "2" was selected to supply the sonicator. To load the sonicator with solution, a 50 mL syringe was attached via a tube. This syringe was filled with the desired solution, which will be discussed shortly. To control the syringe rate of flow, the syringe was installed onto a syringe pump with a flow rate set to 9 mL/min. Finally, one or more substrates were chosen and heated in an oven to 100 °C. Once heated, the ultrasonic power supply and syringe pump were turned on and the spray was applied to the substrate for approximately 2 seconds while inside of the oven. Figure 5.2 shows the overall experimental setup.

Figure 5.1: Atomizer nozzle attached to an ultrasonic power supply and syringe with a syringe pump.

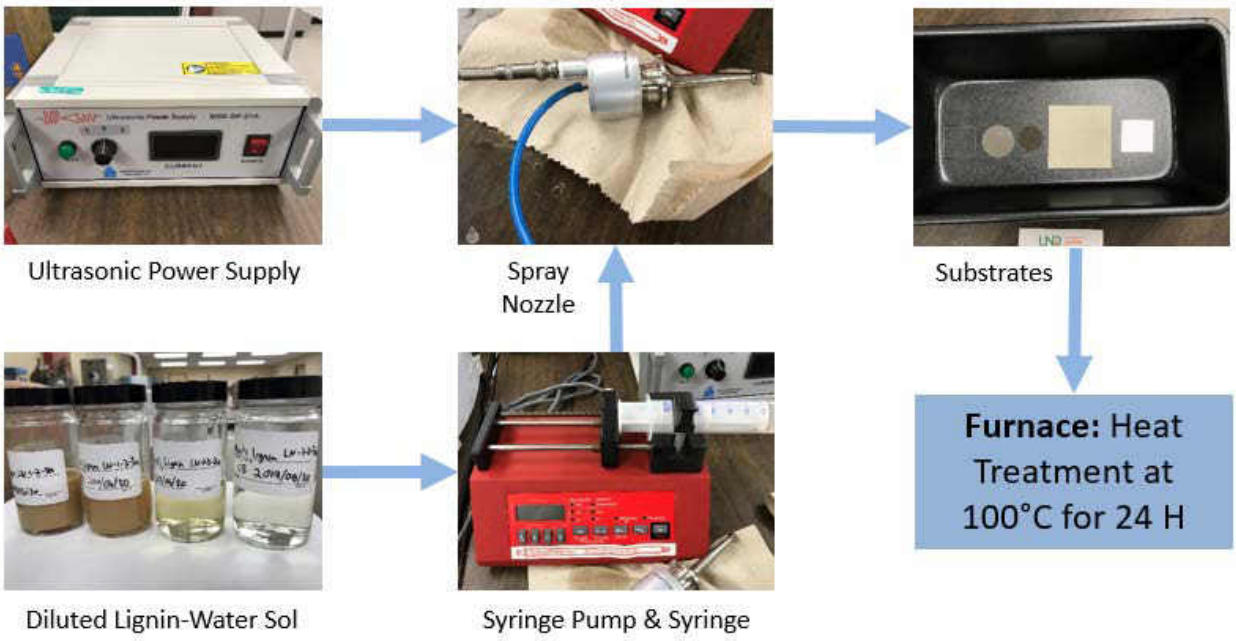

Figure 5.2: Experimental setup to deposit LNPs with an ultrasonicator.

5.2.2 Design Matrix

Four different concentrations of precipitated lignin were used, named LN1-2-3b, LN1-2-3a, LN1-3-2a, and LN1-3-1a. The composition of these concentrations has not been reported since this work is still in progress. Each solution was sprayed for 2 seconds onto a preheated polished aluminum stud at 100 °C while in an oven set to 100 °C.

5.3 Discussion and Future Work

During SEM analysis, no particles were identifiable thus the results were inconclusive. We believe that the solutions used in the experiment were too diluted and the amount of exposure time of ultrasonic spraying onto the substrate was not sufficient. For these reasons, this work is not complete and has been identified as future work for the time being. Our current challenge is being able to spray a solution diluted enough that the LNPs remain in the nano-range, but are prevalent enough to characterize with an SEM.

Other future work includes further characterization of lignin. Determining the molecular weight may be helpful for identifying composites lignin would effectively reinforce. Gel permeation chromatography (GPC) is one approach that may be used to accomplish obtaining the molecular weight of lignin-acetone solution. Another characterization methodology of interest is small-angle x-ray scattering (SAXS). This would allow larger particle sized samples to be analyzed. A third characterization method of interest is atomic force microscopy (AFM). This would help us better understand lignin agglomeration and surface interactions.

Additionally, it would be useful to further investigate the potential to coat glass surfaces with lignin. Tribological surface behavior may be further studied to determine the effectiveness of lignin coatings.

REFERENCES

[1] Guern, Claire Le. "Plastic Pollution." When the Mermaids Cry: The Great Plastic Tide. Coastal Care, 31 Jan. 2020. Web. 31 July 2020.

[2] "Our Planet Is Drowning in Plastic Pollution. This World Environment Day, It's Time for a Change." #BeatPlasticPollution This World Environment Day. UN Environment, 2018. Web. 31 July 2020.

[3] Butler, Adam. "Do Customers Really Care About Your Environmental Impact?" Forbes. Forbes Magazine, 21 Nov. 2018. Web. 31 July 2020.

[4] Tian, Dong, Jinguang Hu, Jie Bao, Richard P. Chandra, Jack N. Saddler, and Canhui Lu. "Lignin Valorization: Lignin Nanoparticles as High-value Bio-additive for Multifunctional Nanocomposites." Biotechnology for Biofuels 10.1 (2017).

[5] Azadi, Pooya, Oliver R. Inderwildi, Ramin Farnood, and David A. King. "Liquid Fuels, Hydrogen and Chemicals from Lignin: A Critical Review." Renewable and Sustainable Energy Reviews 21 (2013): 506-23.

[6] Duval, Antoine, and Martin Lawoko. "A Review on Lignin-based Polymeric, Micro- and Nano-structured Materials." Reactive and Functional Polymers 85 (2014): 78-96.

[7] Jiang, C., H. He, H. Jiang, L. Ma, and D. M. Jia. "Nano-lignin Filled Natural Rubber Composites: Preparation and Characterization." Express Polymer Letters 7.5 (2013): 480-93.

[8] Liu, C., Y. M. Li, and Y. Hou. "Preparation and Structural Characterization of Lignin Micro/nano-particles with Ionic Liquid Treatment by Self-assembly." Express Polymer Letters 12.10 (2018): 946-56.

[9] Goliszek, M., B. Podkościelna, K. Fila, A. V. Riazanova, S. Aminzadeh, O. Sevastyanova, and V. M. Gun'Ko. "Synthesis and Structure Characterization of Polymeric Nanoporous Microspheres with Lignin." Cellulose 25.10 (2018): 5843-862.

[10] Sohni, Saima, Rokiah Hashim, Hafiz Nidaullah, Junidah Lamaming, and Othman Sulaiman. "Chitosan/nano-lignin Based Composite as a New Sorbent for Enhanced Removal of Dye Pollution from Aqueous Solutions." International Journal of Biological Macromolecules 132 (2019): 1304-317.

[11] Christopher, Lew Paul, Bin Yao, and Yun Ji. "Lignin Biodegradation with Laccase-Mediator Systems." Front. Energy Res., 31 (2014), https://doi.org/10.3389/fenrg.2014.00012.

[12] Gupta, Surojit, Maharshi Dey, Sabah Javaid, Yun Ji, and Scott Payne. "On the Design of Novel Biofoams Using Lignin, Wheat Straw, and Sugar Beet Pulp as Precursor Material." ACS Omega 5, 1707-1708 (2020).

[13] Yang, Weijun, Jose M. Kenny, and Debora Puglia. "Structure and Properties of Biodegradable Wheat Gluten Bionanocomposites Containing Lignin Nanoparticles." Industrial Crops and Products 74 (2015): 348-56.

[14] Roopan, Selvaraj Mohana. "An Overview of Natural Renewable Bio-polymer Lignin towards Nano and Biotechnological Applications." International Journal of Biological Macromolecules 103 (2017): 508-14.

[15] Anwer, Muhammad A.S., Hani E. Naguib, Alain Celzard, and Vanessa Fierro. "Comparison of the Thermal, Dynamic Mechanical and Morphological Properties of PLA-Lignin & PLA-Tannin Particulate Green Composites." Composites Part B: Engineering 82 (2015): 92-99.

[16] Gordobil, Oihana, Rafael Delucis, Itziar Egüés, and Jalel Labidi. "Kraft Lignin as Filler in PLA to Improve Ductility and Thermal Properties." Industrial Crops and Products 72 (2015): 46-53.

[17] Aldam, Saud Abu, Maharshi Dey, Sabah Javaid, Yun Ji, and Surojit Gupta. "On the Synthesis and Characterization of Polylactic Acid, Polyhydroxyalkanoate, Cellulose Acetate, and Their Engineered Blends by Solvent Casting." Journal of Materials Engineering and Performance March (2020). https://doi.org/10.1007/s11665-020-04594-3.

[18] Gupta, Surojit, Maharshi Dey, Caleb Matzke, Grant Ellis, Sabah Javaid, Kathryn Hall, Yun Ji, and Scott Payne. "Synthesis and Characterization of Novel Foams by Pyrolysis of Lignin." January 2019 TAPPI Journal 18.01 (2019): 45-56.

[19] Janigová, Ivica, Igor Lacík, and Ivan Chodák. "Thermal Degradation of Plasticized Poly(3-hydroxybutyrate) Investigated by DSC." Polymer Degradation and Stability 77.1 (2002): 35-41.

[20] Technical Note: Intensity - Volume - Number, Which Size Is Correct? N.p.: Malver Instruments Limited, 2017.

[21] Joseph, Emil, and Gautam Singhvi. "Multifunctional Nanocrystals for Cancer Therapy: A Potential Nanocarrier." Nanomaterials for Drug Delivery and Therapy (2019): 91-116.